

REVIEW

[View Article Online](#)
[View Journal](#) | [View Issue](#)



Cite this: *Mater. Chem. Front.*,
2023, 7, 4880

Metal–organic framework-based SERS sensing platforms for life and health detection

Lindong Ma, Meihui Liu, Xinyuan Zhou, Cancan Li and Tie Wang  *

Advancements in life and health detection technology can greatly improve early disease diagnosis and treatment options for patients. Surface-enhanced Raman scattering (SERS) technology has become a preferred method for life and health detection due to its numerous advantages over traditional detection methods. However, the construction of SERS substrates with high sensitivity, selectivity, and repeatability remains a challenge. To overcome these challenges, metal–organic frameworks (MOFs) have emerged as promising solutions because of their unique structures and functions. The design and construction of MOF-based SERS sensing platforms with specific structures and functions are crucial to achieving the goal of life and health detection. This review outlines the synthesis strategies for MOF-based SERS substrates with various structures and functions and highlights the unique roles and performances of MOFs in SERS sensing platforms. During the detection process, MOFs can enrich trace target molecules to enhance detection sensitivity, capture selectively target molecules to improve specificity, exhibit synergistic effects to increase detection signal intensity and improve detection reproducibility and stability. Furthermore, this review explores the applications of MOF-based SERS sensing platforms in life and health detection, including breath analysis, fluid detection, and bioimaging. Finally, the challenges and opportunities faced by MOF-based SERS sensing platforms are discussed in the field of life and health detection, as well as their trend toward miniaturization and intelligentization. With continuous research and development, MOF-based SERS sensing platforms are poised to become a cornerstone of life and health monitoring in the future.

Received 27th April 2023,
Accepted 3rd July 2023

DOI: 10.1039/d3qm00471f

rsc.li/frontiers-materials

1. Introduction

Life and health detection refers to a series of testing methods used to check the health status of an individual. This can include biochemical analysis, blood tests, imaging scans, and more.^{1–3} The goal is to prevent diseases, improve quality of life, and detect and treat potential health problems early on. Currently, life and health detection plays a crucial role in diagnosing and treating illnesses, as well as monitoring patients during recovery.^{4,5} First, life and health detection helps people understand their health status so that they can take better preventive measures and manage their health to avoid serious diseases. Second, it can help people optimize their lifestyles, change unhealthy habits, and improve their overall health levels. Finally, life and health detection can provide physicians with better medical evidence to help them develop more personalized and scientifically based treatment plans. Today, life and health detection has become increasingly popular and recognized. More and more people are paying attention to their

physical health and actively undergoing life and health detection to detect diseases early and prevent or treat them as soon as possible.⁶ However, there are also some problems with health and wellness screening, such as inaccurate results, lengthy testing times, and the potential negative effects of too many tests. Raman spectroscopy technology, particularly SERS detection technology, is especially attractive in the field of life and health detection and analysis.^{7,8} It offers significant advantages, including high sensitivity, non-invasiveness and the ability to provide real-time measurements. With further research and development, Raman spectroscopy could potentially revolutionize the way we approach life and health detection.

Traditional Raman spectroscopy has several limitations, including low sensitivity, weak signals, poor reproducibility, and susceptibility to fluorescence background interference, which restrict its application.⁹ To overcome these limitations, researchers have been exploring new Raman detection technologies. The emergence of SERS has significantly improved the sensitivity of Raman spectroscopy analysis and has thus been widely used in various analytical detection fields.¹⁰ SERS is a highly sensitive vibrational spectroscopy technique that combines Raman spectroscopy with plasmonic materials that

Tianjin Key Laboratory of Life and Health Detection, Life and Health Intelligent Research Institute, Tianjin University of Technology, Tianjin 300384, China.
E-mail: wangtie@email.tjut.edu.cn

exhibit electromagnetic enhancement effects.^{9,11,12} The plasmonic substrates can enhance the Raman signal, making it particularly useful for detecting trace targets. This enhancement provides many benefits, including detection sensitivity and accuracy. The effectiveness of SERS depends mainly on the substrates of SERS, typically composed of plasmonic nanoparticles or nanostructured surfaces with strong surface plasmon resonance. In addition, the target analyte must be close to the SERS hotspots to obtain a strong signal. Designing and synthesizing SERS substrates with high Raman signal enhancement is crucial to building a powerful SERS sensing platform.^{13,14} Although some SERS platforms meet specific requirements such as reproducibility, stability, and sensitivity, existing SERS substrates have difficulties handling low concentrations, high speed flow, and complex real samples due to insufficient affinity between the plasmonic surface and the analytes and other molecular interferences.^{15,16} These problems seriously hinder the widespread application of SERS in life and health detection. Therefore, there is an urgent need for new materials to construct high-performance SERS sensing platforms for life and health detection.

Materials science has played an important role in the advancement of analytical and detection technologies by developing advanced materials to improve sensitivity, selectivity, and reproducibility.^{17,18} MOFs, or metal-organic frameworks, are a class of crystalline porous materials composed of metal ions and organic ligands that can be designed and synthesized to overcome these challenges.^{19–21} MOFs possess excellent properties such as good stability, a large surface area and porosity, a uniform nano-level cavity structure, and functionalized modification on both inner and outer surfaces, making them ideal for analysis and detection.^{22–25} In particular, MOFs have gained attention in the field of SERS technology due to their outstanding performance characteristics, including strong affinity for target molecules, molecular sieving effects, and stability in complex environments. By integrating plasmonic nanoparticles into MOFs, researchers can construct MOF-based SERS sensing platforms that offer inherent advantages in improving SERS for life and health detection. For example, the large specific surface area, tunable pore size and easy modification and functionalization of MOFs can effectively enrich and selectively capture trace analytes in complex systems.^{26–29} Overall, introducing MOFs to prepare high-performance MOF-based SERS sensing platforms has been proven to be an effective method to overcome the current bottleneck of SERS and improve its capabilities in analysis and detection.

MOFs have emerged as a promising solution for overcoming the challenges faced by traditional SERS sensing platforms in SERS detection. Researchers widely recognize the crucial role of MOF-based SERS sensors in analysis and detection. As these platforms continue to be designed and prepared, their advantages and opportunities become increasingly apparent. While some review articles have examined the development of MOF-based SERS sensing platforms, they lack a detailed overview of MOF-based SERS sensing platforms in life and health detection.^{30–34} This article primarily reviews the latest progress

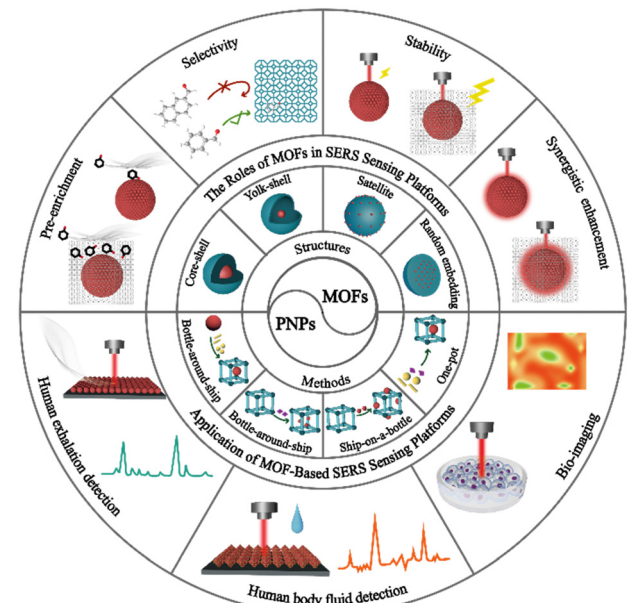


Fig. 1 Schematic diagram of MOF-based SERS sensing platforms for life and health detection.

of MOF-based SERS sensing platforms, highlights the significant role of MOFs in MOF-based SERS sensing platforms and discusses their applications in life and health detection (Fig. 1). First, we classify and summarize the synthesis strategies and structures of MOF-based SERS substrates. Next, we elaborate on the unique roles and detection performance of MOFs in SERS sensing platforms, such as enriching trace target molecules to improve detection sensitivity, selectively capturing target molecules to improve specificity, synergistic effects to increase detection signal intensity, and improving detection reproducibility and stability, combined with classical examples. Then, we explore the application of MOF-based SERS sensing platforms in life and health detection, including exhalation detection, body fluid detection, and biological imaging. Finally, we discuss the challenges and opportunities faced by MOF-based SERS sensing platforms in life and health detection, and their future development trends towards miniaturization and intelligence. This review aims to encourage further advancement of MOF-based SERS sensing platforms in the field of life and health detection.

2. Preparation of MOF-based SERS sensing platforms for life and health detection

In the field of life and health analysis and detection, it is crucial to construct high-performance MOF-based SERS sensing platforms. Therefore, taking into consideration the complexity of the detection matrix and the composition of target molecules, various preparation strategies should be implemented to design the structure and function of MOF-based SERS substrates rationally. The integration of PNPs with MOFs to

create composite materials has significant potential to construct SERS sensing platforms for life and health detection.^{35–39} PNPs/MOFs composite materials have been found to exhibit SERS enhancement effects higher than those of unmodified MOFs, highlighting the importance of rational design and synthesis of these composites for future applications in the field of life and health detection. To better understand these materials, researchers have classified PNPs/MOFs composite materials into four main categories based on their structures: core–shell,¹⁴ yolk–shell,^{40,41} satellite^{42,43} and randomly embedded structures.^{44–46} The synthesis strategy for confining PNPs within MOFs has also matured and can be broadly classified into four types: a bottle-around-ship strategy, ship-in-a-bottle strategy, ship-on-a-bottle strategy, and one-pot strategy.⁴⁷ Overall, these advances in PNPs/MOFs composite materials offer exciting possibilities in life and health detection through the creation of effective SERS substrates. Further research and development in this area may lead to innovative applications and improvements in healthcare diagnostics.

2.1 Bottle-around-ship strategy

The “bottle-around-ship” strategy is commonly used to produce SERS sensing platforms for life and health monitoring.⁴¹ This process involves two main steps. Firstly, PNPs are prepared. Secondly, pre-made PNPs are added to a MOF precursor solution as seeds or nucleation centers. This induces the growth or assembly of MOFs around the PNPs, resulting in the formation of PNPs/MOFs structures. This method primarily yields core–shell structured PNPs/MOFs SERS substrates that offer several benefits. First, by encapsulating PNPs within the MOF shell, the migration and agglomeration of nanoparticles (NPs) can be significantly restricted, enhancing substrate stability. Second, the thickness of MOFs and the size, shape, composition, and position of PNPs can be precisely controlled and designed. Finally, MOFs achieve high porosity, a large specific surface area, and high density of reactive sites. As a result, PNPs/MOFs SERS substrates have provided new opportunities to create highly sensitive, reproducible, and selective SERS sensing platforms.

In this method of synthesizing MOFs, the presence of capping agents or surfactants on the surface of PNPs plays a vital role. These agents provide interaction sites for the synthesis of MOFs, with the PNPs serving as heterogeneous nucleation centers, which to some extent suppress the spontaneous formation of MOFs in solution. A common approach is to introduce “binders” such as polyvinyl pyrrolidone (PVP) and cetyltrimethylammonium bromide (CTAB) to modify PNPs, thereby facilitating the growth and nucleation of MOFs on their surfaces.⁴⁹ For instance, Huo and his team reported a controllable encapsulation strategy in which PVP-stabilized NPs of varying sizes, shapes, and compositions were encapsulated within ZIF-8, resulting in well-dispersed and fully encapsulated NPs within the ZIF-8 framework (Fig. 2A).⁴⁸ This strategy involved functionalizing the surface of the NPs with PVP and optimizing the crystallization of ZIF-8. Under optimized experimental conditions, core–shell-structured NPs@MOFs

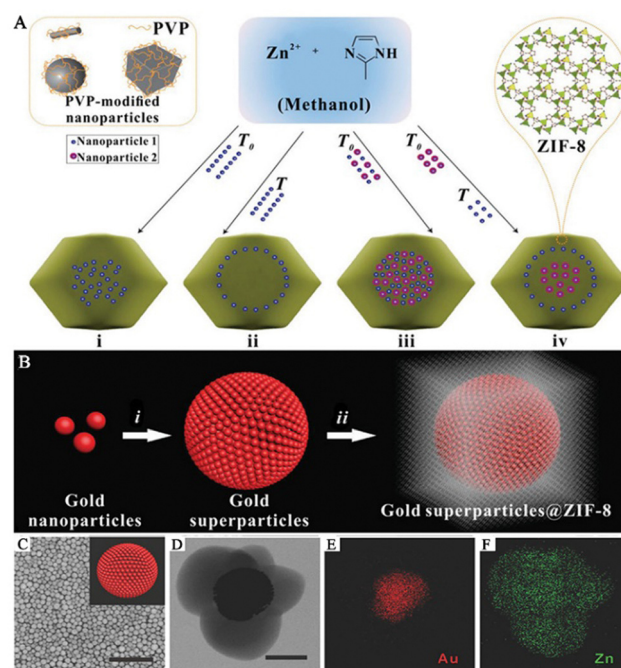


Fig. 2 Composite materials of PNPs/MOFs with core–shell structure. (A) A schematic diagram of a controlled encapsulation strategy to prepare NPs@ZIF-8.⁴⁸ Reproduced with permission from Springer Nature, copyright 2012. (B) A schematic diagram of the preparation of GSPs@ZIF-8. Scale bar: 1 μ m. (C) SEM image of the GSPs. Inset: the schematic diagram of GSPs. (D) TEM image of the GSPs@ZIF-8. Scale bar: 100 nm. (E and F) Energy-dispersive X-ray elemental map of GSPs@ZIF-8.¹⁴ Reproduced with permission from John Wiley and Sons, copyright 2018.

composite materials were prepared by crystallizing ZIF-8 in the presence of PVP-modified NPs in methanol. This strategy works for a wide range of NPs, allowing various NPs to be incorporated without aggregation and controlling their spatial distribution within the MOF shells, thereby opening up new avenues for the use of NPs@MOFs composite materials as SERS sensing platforms. Wang and his team have successfully synthesized gold superparticles (GSPs) that possess the ability to self-assemble into spherical shapes.¹⁴ These GSPs were then encapsulated with ZIF-8 to create core–shell structures called GSPs@ZIF-8, which serve as excellent substrates for surface-enhanced Raman scattering (Fig. 2B). The production of GSPs was accomplished *via* a revised technique for assembling microemulsions with water-in-oil (W/O). In this method, the hydrophobic bonds linking the oil amine on the AuNPs with the alkyl chains of dodecyl trimethyl ammonium bromide (DTAB) were weakened to generate superparticles that possess SERS “hot spots”. (Fig. 2C). PVP was introduced to stabilize GSPs in different solvents and promote the growth of MOF shells. A ZIF-8 shell with a thickness of approximately 150 nm was coated on a single GSP core to form GSPs@ZIF-8 (Fig. 2D). Ionic surfactants such as DTAB were used to adjust the surface of superparticles to minimize the energy required for MOF nucleation and growth, thereby suppressing the uniform crystal growth of ZIF-8. Energy-dispersive X-ray elemental mapping revealed that Zn was evenly distributed throughout the

nanostructure, while Au was concentrated in the core (Fig. 2E and F). Meanwhile, Li and his team showed that by controlling the volume and concentration of the precursor, different core-shell Au@ZIF-8 and their structures could be obtained.³⁹ For example, the addition of organic ligand dimethylimidazole to a low concentration gold solution could precisely prepare nanostructures with different shell thicknesses (3–50 nm) by adjusting the amount of Zn²⁺ and 2-methylimidazole added. On the other hand, adding the organic ligand dimethylimidazole to a high-concentration gold solution can control the formation of multi-core-shell structures, leading to better control of the distance between AuNPs.

To establish a highly effective SERS sensing platform for the accurate detection of biomarkers, many research teams have developed MOF-based SERS substrates with yolk-shell structure. These yolk-shell SERS substrates can effectively eliminate interference from other components and have lower detection limits compared to core-shell structured SERS substrates. The hollow MOF shells in these substrates enrich more gas molecules and the enriched molecules come into contact or react with the surface of PNPs, producing strong SERS signals. For example, Wang and his team prepared a hollow Co-Ni layered double hydroxide (LDH) nanocage on Ag nanowires (Ag@LDH) (Fig. 3A).⁴¹ They accomplished this by preparing a hollow Co-Ni LDH nanocage to adsorb gas molecules, resulting in SERS

sensing platforms based on Ag@LDH. In the first step, 2-methylimidazole nucleated with Co²⁺ ions on the surface of polyvinylpyrrolidone-modified Ag nanowires and continued to grow to form an Ag@ZIF-67 composite material (Fig. 3C). In the second step, ion etching of the metal-organic framework transformed it into a cobalt–nickel-layered double metal hydroxide with a nanocage structure, forming an Ag@Co-Ni LDH composite material (Fig. 3D). Similarly, to precisely identify the biomarkers present in exhaled breath and remove any obstacles from other components, Wang and his team proposed employing hollow ZIF-8 that encloses GSPs that possess yolk-shell structures as the SERS substrate (GSPs@H-ZIF-8).⁴⁰ The team fabricated a composite material with yolk-shell structures by incorporating GSPs into a hollow ZIF-8 framework, which was formed using tannic acid (Fig. 3E). The PVP-stabilized GSPs were introduced into a solution containing ZIF-8 precursors, resulting in the formation of a GSPs@ZIF-8 composite material (Fig. 3G). Subsequently, the interior of the ZIF-8 was etched with tannic acid, leading to the creation of a hollow layer of ZIF-8 that preserved the structure of the framework (Fig. 3H).

Using the “bottle-around-ship” strategy, researchers have successfully synthesized SERS substrates with both core-shell and yolk-shell structures, which have important applications in the field of life and health detection. While both structures are commonly used in SERS-based detection, they also have their own advantages and disadvantages. One advantage of the core-shell SERS substrate is that it can provide good SERS activity and aggregated PNPs can form a porous structure, further enhancing the SERS signal. For instance, compared to bare GSPs, the GSPs@ZIF-8 structure synthesized using the “bottle-around-ship” strategy can offer a larger hot spot field.¹⁴ Another advantage is that MOFs, as a new class of nanomaterials, have a controllable pore size, highly structured and detailed surface chemical properties, and can protect PNPs from contamination by encapsulation. Thus, under the protection of the MOFs’ shells, PNPs can maintain their stability and repeatability during life and health monitoring, thereby improving the accuracy and reliability of SERS detection. The core-shell SERS substrate can also adjust its SERS performance by controlling the composition, shape, and size of the nanomaterials, achieving selective detection and quantitative analysis of the target molecules. Additionally, the large specific surface area and adjustable pore size of the MOF shell allow molecules to diffuse to the surface of the SERS substrate, thereby improving the detection sensitivity. However, there are also some limitations to the core-shell SERS substrate, such as the complex synthesis steps and high preparation cost, because of the need to modify the MOFs’ shell on the surface of PNPs. The encapsulation of the MOFs’ shell may also reduce the contact between PNPs and samples, weakening the SERS signal. Furthermore, the addition of the MOFs’ shell may lower the SERS sensitivity of the metal NPs since the MOFs’ shell can absorb some laser energy and inhibit Raman scattering. However, researchers can reduce this signal attenuation by adjusting the composition of the MOFs’ shell, such as controlling parameters like the thickness of the MOFs, the size of the pores

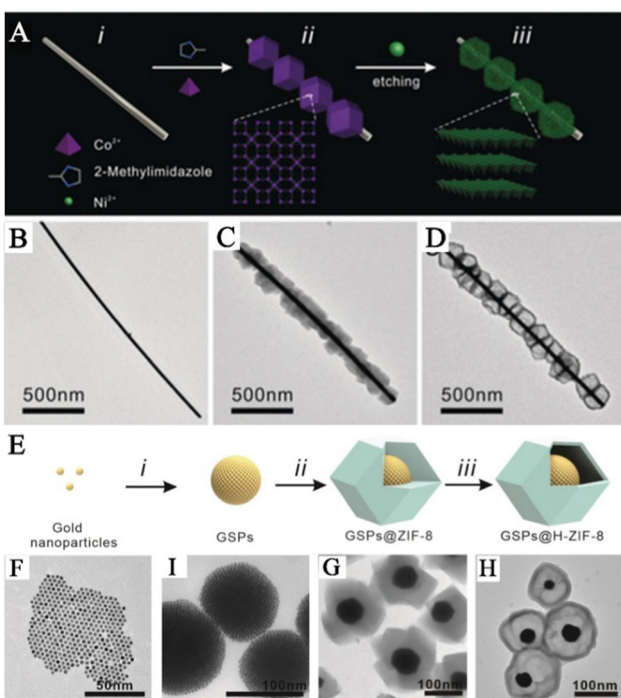


Fig. 3 Composite materials of PNPs/MOFs with yolk-shell structure. (A) Schematic diagram of the synthetic pathway of Ag@LDH. (B) TEM image of Ag nanowires. (C) TEM image of Ag@ZIF-67. (D) TEM image of Ag@LDH.⁴¹ Reproduced with permission from John Wiley and Sons, copyright 2019. (E) Schematic diagram of the synthetic pathway of GSPs@H-ZIF-8. (F) TEM image of AuNPs. (I) TEM image of GSPs. (G) TEM image of GSPs@ZIF-8. (H) TEM image of GSPs@H-ZIF-8.⁴⁰ Reproduced with permission from John Wiley and Sons, copyright 2022.

and the chemical composition to improve the SERS response. Compared to other SERS substrates, yolk shell structures offer some distinct advantages. First, the PNPs in these structures are enclosed within the porous shell layer of MOFs. This layer provides a larger surface area for adsorbing target molecules and can help aggregate these molecules around PNPs, thereby strengthening the SERS signal intensity. For instance, the hollow structure of Ag@LDH synthesized using the “bottle-around-ship” strategy mitigates the diffusion limitation of the original MOF microporous structure for target molecules, thus increasing the detection sensitivity.⁴¹ This is particularly useful for capturing and detecting trace gas molecules in exhaled breath. Second, the proximity between PNPs in the yolk shell structures and target molecules is greater, leading to a significant boost in SERS signal intensity due to near-field effects. As a result, SERS substrates with yolk shell structures can achieve higher sensitivity and lower detection limits. However, there are some drawbacks to using yolk-shell structures as SERS substrates. Their fabrication processes are complex and expensive, and they are less stable than core-shell structure SERS substrates, making them susceptible to environmental factors that could affect their performance unpredictably. Therefore, it is essential to choose the appropriate SERS substrate based on the specific application requirements. To develop high-performance SERS sensing platforms for life and health detection, further exploration of PNPs/MOFs with better performance is necessary.

2.2 Ship-in-a-bottle strategy

The approach of incorporating PNPs inside the preexisting pores or cavities of MOFs to achieve reduction is commonly known as the “ship-in-a-bottle” strategy.^{50,51} This method involves encapsulating the precursor of PNPs in MOF cavities and consequentially obtaining composite structures of PNPs/MOFs by means of subsequent reduction treatment. The technique is simple and efficient, and small-sized PNPs can be utilized as seeds to grow large-sized PNPs. Additionally, hosting PNP guests within MOF structures restricts their migration and aggregation, significantly improving the stability of SERS substrates.⁵² Different techniques such as solution impregnation^{53,54} and double solvents are available, relying on the introduction of metal precursors. Despite some progress, precisely controlling the location, size, and shape of PNPs in MOFs through the employment of the “ship-in-a-bottle” strategy remains a challenging task.

In the conventional impregnation reduction process, confining PNPs inside the pores of MOFs and preventing their aggregation on the exterior surface of MOFs pose significant challenges. Cao and his team effectively utilized an impregnation approach to synthesize MOFs decorated with AuNPs, resulting in enhanced SERS performance (Fig. 4A).⁵³ Artificially created composite materials made up of AuNPs/MOFs exhibit localized surface plaque resonance (LSPR) characteristics and possess a significant adsorption capacity of MOFs. This ability enables the preconcentration of analytes in close proximity to the surface of AuNPs, leading to outstanding SERS

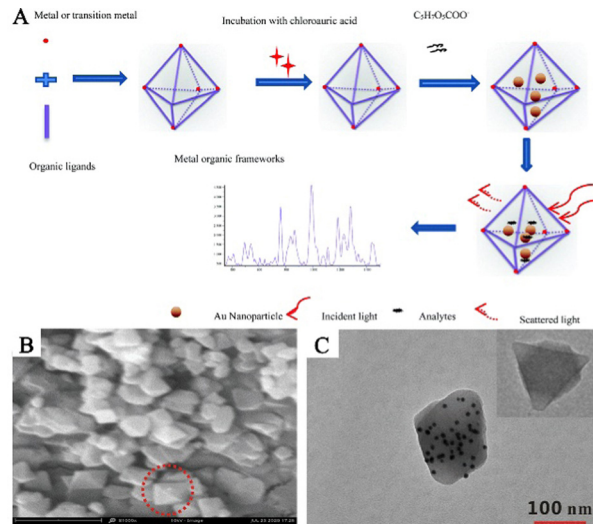


Fig. 4 The randomly embedded PNPs/MOFs composites were synthesized by solution impregnation. (A) Schematic diagram of the synthesis process of AuNPs/MOFs composites for the determination of an analyte.⁵³ Reproduced with permission from the Royal Society of Chemistry, copyright 2017. (B) SEM image of AuNPs/AE-MIL-101 (Cr). (C) TEM image of AuNPs/AE-MIL-101 (Cr). Inset: TEM images of AE-MIL-101 (Cr).⁵⁴ Reproduced with permission from Springer Nature, copyright 2021.

performance. This work lays the foundation for the preparation of PNPs/MOFs composite materials as high-performance SERS sensing platforms for life and health detection by utilizing a simple solution impregnation strategy. Feng and his team prepared an AuNPs/AE-MIL-101(Cr) composite material *via* a solution impregnation method (Fig. 4B and C).⁵⁴ In this strategy, the pore structure of the MIL-101(Cr) composite material was optimized by phosphoric acid etching, which widened its pore size distribution and made PNPs more accessible to the interior of MOFs. The AuNPs were embedded in acid-etched (AE)-MIL-101(Cr) to prepare the AuNPs/AE-MIL-101(Cr) composite material. By combining the prepared AuNP/AE-MIL-101(Cr) composite material with an enzyme-linked immunosorbent assay (ELISA), a SERS sensing platform was constructed and successfully used to determine human carboxylesterase 1 (HCE1) in plasma from patients with hepatocellular carcinoma (HCC), showing good clinical application potential.

The dual solvent method is an effective technique that overcomes the limitations of traditional impregnation methods and prevents the generation of PNPs and the aggregation on the outer surfaces of the MOFs. In this method, a solution containing the metal precursors and MOF materials is thoroughly mixed. The capillary effect of the MOF pores enables the metal precursor solution to penetrate spontaneously into the internal pores of the MOFs. The reducing agent then converts the metal precursor solution into PNPs, resulting in PNPs/MOFs composite materials. Hu and his team used this strategy to prepare AuNPs@MIL-101 composite materials to construct a SERS sensing platform that detects glucose and lactate in tissues (Fig. 5A and B).⁵⁵ They fully mixed MIL-101 with H₄AuCl₄ solution and prepared AuNPs using a sodium citrate solution

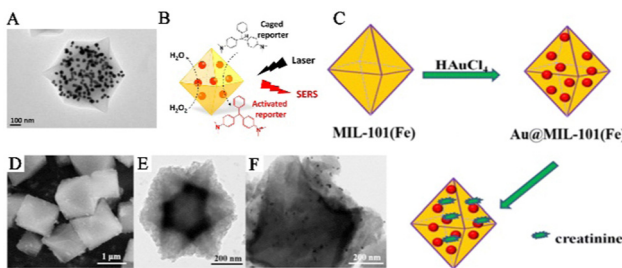


Fig. 5 The randomly embedded PNPs/MOFs composites were synthesized using a dual solvent method. (A) TEM image of AuNPs@MIL-101. (B) Schematic illustration of AuNPs@MIL-101 acting as a SERS substrate.⁵⁵ Reproduced with permission from American Chemical Society, copyright 2017. (C) *In situ* construction process of Au@MIL-101(Fe). (D) SEM image of MIL-101(Fe). (E and F) TEM images of MIL-101(Fe) and Au@MIL-101(Fe).⁵⁶ Reproduced with permission from World Scientific Publishing Co Pte Ltd, copyright 2021.

as the reducing agent. After a centrifugation treatment, the AuNPs@MIL-101 composite materials were obtained. These composite materials not only act as peroxidase mimetics that catalyze the conversion of non-Raman active reporters into Raman-active reporters but also enhance the Raman signal of active reporters as SERS-active substrates. Furthermore, the team further modified the AuNPs@MIL-101 composite materials by oxidases, creating AuNPs@MIL-101@oxidase-integrated nano-enzymes that measured changes in glucose and lactate related to ischemic stroke in live animal brains. Similarly, Jiang and his team synthesized Au/MIL-101(Fe) SERS substrates with good anti-interference properties by mixing pre-synthesized MIL-101(Fe) with different concentrations of chloroauric acid to allow metal precursors to fully enter MIL-101(Fe) (Fig. 5C–F).⁵⁶ They rapidly added a sodium citrate solution to prepare the AuNPs. The team constructed a SERS sensing platform to monitor creatinine in urine using the AuNPs@MIL-101 composite materials. The electrostatic interaction between the MIL-101(Fe) framework and creatinine brought it close to the SERS hotspots, significantly enhancing the SERS signal.

Using the “bottle-around-ship” strategy, a SERS substrate with a randomly embedded structure was successfully synthesized. The SERS substrates with random embedding structures are commonly used and have the following advantages and disadvantages: (1) compared to core-shell structured SERS substrates, the SERS substrates with random embedding structures are easier to prepare. (2) Due to their complex morphology and high surface roughness, the SERS substrates with random embedding structures can provide very high SERS enhancement effects, resulting in higher sensitivity. (3) The SERS substrates with random embedding structures can be used for various types of targets (including liquids and gases) in life and health detection, making them widely applicable. However, there are also disadvantages in using the SERS substrates with random embedding structures: (1) since their morphology is uncertain, their SERS signals may fluctuate significantly, leading to signal instability. (2) It is difficult to precisely control the size, quantity, and distribution of PNPs within MOFs on SERS

substrates with random embedding structures, making their preparation process relatively uncontrollable and challenging for batch production and repeat manufacturing. (3) When PNPs are embedded in MOFs, pore blockage may occur, making it difficult for target molecules to reach the SERS hotspots and thus reducing the performance of the SERS sensors.

2.3 Ship-on-a-bottle strategy

A satellite-structured SERS substrate is a unique structure that differs from the core-shell-structured SERS substrate. In this structure, PNPs are assembled on the surface of MOFs to create a satellite-structured SERS composite material.^{42,57} The reduction of PNPs *in situ* on pre-synthesized MOFs to preserve their inherent crystallinity is carried out similar to the immersion strategy. This method is called the “ship-on-a-bottle” strategy.⁵⁸ Typically, a reductant is selectively applied to the surface of MOFs to facilitate the reduction of metal salts and the subsequent formation of metal NPs. The unique structure of MOFs provides an ultrahigh surface area and enables the attachment of numerous SERS-active PNPs. The metal NPs are fixed on the outer surface of the MOFs and a large number of stable and uniform SERS hotspots can be formed. As a result, the generated composite material combines the SERS performance of PNPs with the adsorption capacity of MOFs, making it an excellent SERS substrate for highly sensitive detection of biological signal molecules near the SERS hotspot domains close to PNPs. Compared to SERS substrates where PNPs are encapsulated or embedded in MOFs, SERS substrates where PNPs are anchored on the surface of MOFs exhibit stronger SERS enhancement effects because signal molecules can directly achieve signal enhancement between PNPs and MOFs, causing a large number of “hotspots” to appear at the intersection between PNPs.

For example, Jiang and his team created the SERS substrate AgNPs/MIL-101(Fe) by synthesizing AgNPs *in situ* on the outer surface of MIL-101(Fe) (Fig. 6A and B).⁵⁹ In the early stages, TA was coordinated with the unsaturated hydroxyl group of Fe³⁺ on the surface of MIL-101(Fe) to serve as a reducing agent during

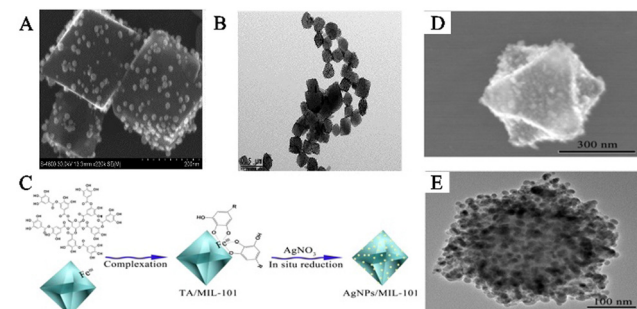


Fig. 6 The satellite PNPs/MOFs composites were synthesized. (A) SEM images of AgNPs/MIL-101(Cr). (B) TEM images of AgNPs/MIL-101(Cr).⁵⁹ Reproduced with permission from American Chemical Society, copyright 2015. (C) Schematic illustration of the preparation of AgNPs/MIL-101(Fe). (D) SEM images of AgNPs/MIL-101. (E) TEM image of AgNPs/MIL-101.⁶⁰ Reproduced with permission from the Royal Society of Chemistry, copyright 2016.

functionalization. As a result, Ag^+ was able to be reduced by TA directly on the surface of MIL-101(Fe), leading to the formation of the composite material AgNPs/MIL-101(Fe). MIL-101(Fe), being a stable host material, provides an ultrahigh surface area and a large number of adsorption sites that enrich guest molecules near the surface of AgNPs, producing strong SERS signals. Furthermore, using the peroxidase-like activity of Fe-MOFs, the obtained AgNPs/MIL-101(Fe) composite material has been used to construct a SERS sensing platform for detecting biological signal molecules such as dopamine (DA). Yang and his team created a new SERS substrate, Ag–Au–MIL-101, which was modified with *para*-amino thiophenol (PATP) for detecting DA in serum.⁶¹ By utilizing the azo reaction between DA and PATP, the detection selectivity was significantly improved. MIL-101 was dispersed in a silver nitrate solution, followed by the addition of trisodium citrate to form an Ag–MIL-101 solution. Then, NH_2OH and HAuCl_4 solutions were added to obtain the Ag–Au–MIL-101 composite material. The porous structure of MIL-101 selectively captured DA molecules, bringing them close to the surface of the MOFs with the PATP reaction sites to produce a strong SERS signal response.

Li and his team designed a novel SERS substrate that combined the remarkable adsorption capacity of MIL-101(Cr) with AgNPs as SERS hotspots (Fig. 6C).⁶⁰ *In situ* synthesis of AgNPs was carried out on the outer surface of MIL-101(Cr) by first initiating the self-polymerization of DA in water to generate polydopamine (PDA), which subsequently was polymerized on the surface of the MOFs. PDA reduced Ag^+ on the surface of MIL-101(Cr), leading to the formation of the satellite structure of AgNPs/MIL-101(Cr) (Fig. 6D and E). AgNPs/MIL-101(Cr) was synthesized, which demonstrated the capacity to capture folic acid (FA) through electrostatic interaction, generating a powerful SERS signal. This led to the creation of a SERS sensing platform that could detect FA in biological samples. The research team has also synthesized many SERS substrates with PNPs anchored on MOF surfaces, including AuNPs/Cu-TCPP,⁶² AgNPs@MOF helical structure,⁶³ AuNPs@MB@HP-UiO-66-NH₂,⁶⁴ TM–Ag@NU-901,⁶⁵ AuNPs@MOFs,^{66,67} and Ag@MIL-101(Cr).⁶⁸

Despite the significant progress made in anchoring PNPs to MOF surfaces as SERS substrates, there are still some challenges that need to be addressed. These challenges include: (1) the relatively high cost of manufacturing satellite-structured SERS substrates, which may hinder their widespread use for life and health detection applications; (2) the complex shape of satellite-structured SERS substrates may make it difficult to achieve directional control and obtain uniform and stable SERS hotspots, which could affect the experimental results; (3) the surface area of satellite-structured SERS substrates is typically smaller than those of other types of SERS substrates, limiting their application in life and health detection; and (4) PNPs located outside the MOF pores pose a challenge in using MOFs as molecular sieves or in studying molecular diffusion kinetics.

2.4 One-pot strategy

The aforementioned synthesis methods provide notable benefits in the design and control of composite materials made of

PNPs/MOFs for SERS sensing platforms employed in life and health detection applications. However, the synthesis process is relatively complex. To address this, researchers have focused on a one-pot strategy as a simple synthesis method to prepare PNPs/MOFs composite materials. This method involves directly mixing metal precursors and MOF precursors to form PNPs/MOFs composite materials that retain SERS hotspot effects. To obtain a flawless composite structure of PNPs/MOFs using the one-pot technique, it is crucial to precisely control the rates of nucleation and growth of PNPs and MOFs. Selecting appropriate organic ligands and solvents is of utmost importance to effectively capture plasma nanoparticle precursors, stabilize resultant PNPs, and promote efficient heterogeneous catalysis of PNPs on the MOF surfaces. However, limitations in reaction conditions make it difficult to control the size, shape, size, and uniformity of obtained PNPs/MOFs composite materials *via* the one-pot synthesis method.

Tang and his team prepared AuNPs@MOF-5 nanocomposites with uniformly shaped and adjustable sizes using the one-pot method.⁶⁹ To prepare core–shell AuNPs@MOF-5, they mixed gold and MOF precursors directly in a reaction solution containing DMF, PVP, and ethanol. The growth rate of AuNPs and MOF-5 can be effectively adjusted by controlling the reaction conditions. Subsequently, MOF-5 grew spontaneously on the surface of PVP-coated AuNPs resulting in the creation of a consistent PVP-stabilized core–shell composite material comprising AuNPs@MOF-5. This work opens a door for constructing SERS substrates for life and health detection in SERS sensing platforms by providing a universal technology for preparing PNPs@MOF composite materials with different types of core–shell structures using the one-pot method. Similarly, Zhang and his team synthesized core–shell Au/MOF-74 composite NPs using a one-step method. The composite material comprising Au@MOF-74 showed outstanding SERS activity, signal reproducibility, and stability. A sensitive detection method for 4-NTP was successfully established based on the Au@MOF-74 composite material.⁷⁰

Although PNPs/MOFs SERS substrates constructed using the one-pot strategy have many advantages, there are still some issues, such as difficulties in forming uniformly distributed SERS “hotspots” with high enhancement efficiency and in controlling the synthesis of MOF shells with different thicknesses and good uniformity after all the reactants are added together. Therefore, more research is needed to develop high-performance SERS sensing platforms for life and health detection using the one-pot strategy.

3. The roles of MOFs in SERS sensing platforms for life and health detection

The development of MOF-based SERS platforms for life and health detection aims to enhance the performance of SERS sensors. To achieve this, it is crucial to recognize the significant role that MOFs play in SERS sensors used for life and health detection. In comparison to traditional SERS substrates, MOFs

possess specific spatial structures in MOF-based SERS sensing platforms, providing several unique advantages for life and health detection. Firstly, the porous structure of MOFs offers adequate surface area and porosity to effectively concentrate target molecules and produce strong SERS signals on their surface, resulting in the highly sensitive detection of trace biological molecules. Secondly, MOFs can act as carriers of PNP, with their pore size and surface functional groups being controllable, allowing PNP to be embedded into the MOF structure. The pore structure and surface chemical properties of MOFs can be utilized for selective recognition and sensitive detection of biological molecules. Thirdly, the synergistic effect of MOFs and PNP can boost SERS signals. This is owing to the high dielectric constants of MOFs, which effectively retard the radial decay of the electromagnetic field, ultimately leading to a substantial improvement in SERS signal intensity in the metal-MOF system. Finally, by encapsulating MOF shells within PNP, the migration and aggregation of PNP can be substantially reduced, thereby enhancing the stability of SERS substrates. In summary, MOFs have a pivotal role in SERS sensors for life and health detection, with promising application prospects.

3.1 MOFs for pre-enrichment of target molecules

The SERS sensing platform faces several challenges in the field of life and health detection, such as the trace concentration of the target analytes,⁷¹ high migration rate⁷² and low affinity with the surface of the PNP.^{73,74} These factors make it difficult to capture and place the analyte effectively on the surface of PNP. However, MOFs have proved to be an effective solution to this problem as they act as adsorbent materials to pre-concentrate the analyte onto the SERS substrate. With their extremely high specific surface area and adjustable three-dimensional pores, MOFs enable the target analyte to diffuse freely through the channels and are highly effective materials for the preconcentration of analytes.^{23,24,75} Through the host-guest interaction between target molecules and MOFs, the trace target analyte can be collected and accumulated effectively on the surface of PNP in MOF-based SERS sensing platforms, thus improving the sensitivity of the SERS sensor. Non-destructive evaluation of volatile organic compounds (VOCs) in exhaled breath poses a significant challenge, but has the potential to serve as a biomarker for the detection of disease in life and health. The electromagnetic enhancement (EM) effect induced by LSPR of PNP (such as gold, silver, and copper) mainly causes SERS.^{76,77} MOFs with powerful adsorption abilities have been used for preconcentration of analytes and further enhancing the SERS signal. Moreover, the significant specific surface area and porous structure of the MOFs enable more efficient enrichment of gas molecules in the SERS hot spot region.

To improve the ability to capture gaseous biomarkers, Wang and his team applied a coating of ZIF-8 onto self-assembled GSPs, which effectively slowed down the flow rate of gaseous molecules and reduced the decay of the electromagnetic field around the surface of the GSPs.¹⁴ The researchers observed significant differences in adsorption between bare GSPs and GSPs@ZIF-8 structures for high-speed moving gaseous

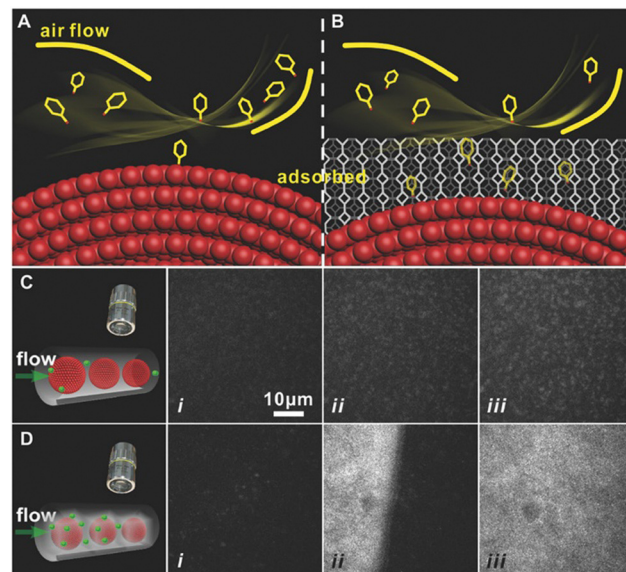


Fig. 7 MOFs for preconcentration of analytes. (A) and (B) Schematic diagrams of the GSPs and GSPs@ZIF-8 with gas collisions. (C) and (D) Total internal reflection fluorescence micrographs of the gas adsorption process on GSPs and GSPs@ZIF-8 at different times.¹⁴ Reproduced with permission from John Wiley and Sons, copyright 2018.

molecules. The collision between these molecules and bare GSPs is close to perfectly elastic, with a very short contact time. After impact, most molecules float away at their original speed without losing kinetic energy (Fig. 7A). The MOF shell of GSPs effectively prolongs the contact time, allowing for increased interaction between gaseous molecules and the porous media (Fig. 7B). This interaction involves both molecular interactions between gas molecules and collisions between gas molecules and the porous medium. An increase in the frequency of collisions between SERS substrates and gaseous molecules means that there is a higher possibility of reaction or absorption in GSPs@ZIF-8 than in GSPs, as immediately observed by total internal reflection fluorescence microscopy (Fig. 7C and D). The researchers were able to quantitatively detect the typical lung cancer biomarker 4-ethylbenzaldehyde in exhaled breath, with a limit of detection (LOD) of 10^{-9} (ppb level).

To detect biomarkers in human breath more sensitively and accurately, Wang and his team prepared hollow Co-Ni LDH nanocages on Ag nanowires to obtain SERS sensors based on Ag@LDH.⁴¹ Silver nanowires offer enhanced Raman signals for detecting trace analytes, while hollow LDH nanocages serve as gas-constrained cavities to enhance capture and adsorption of gaseous analytes. As VOCs pass through the porous LDH medium, the speed in the vicinity of the surface of the silver nanowires alters. Although the tortuosity of the flow path between ZIF-67 and LDH is similar, it is larger than the simulated value using the bare silver nanowire streamline diagram (Fig. 8A). As a result of the dissipation of molecular kinetic energy, gaseous analytes can be effectively adsorbed in both the Ag@ZIF-67 and Ag@LDH models. LDH nanocages possess a unique characteristic of loose, hollow structure and a

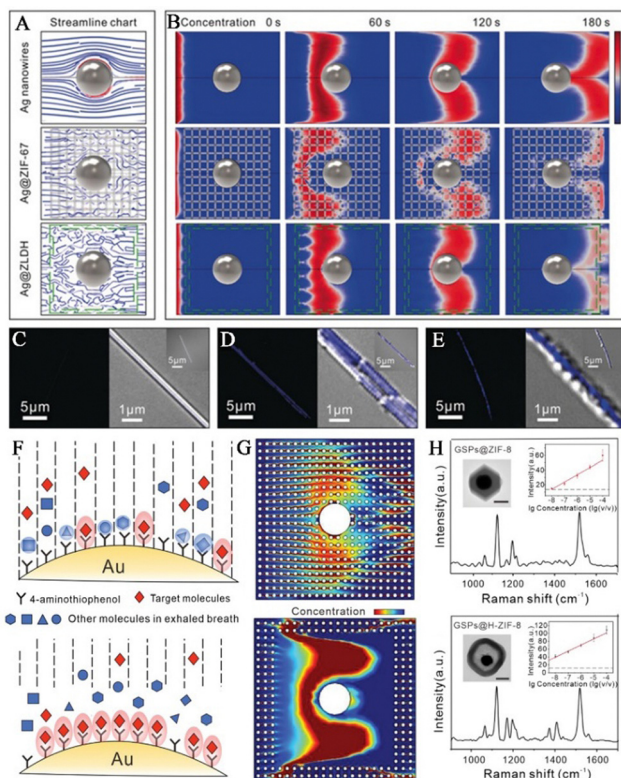


Fig. 8 MOFs for preconcentration of analytes. (A) Simulation streamline graphs of Ag nanowires, Ag@ZIF-67, and Ag@LDH. (B) Modeling fluctuations in the concentrations of Ag nanowires, Ag@ZIF-67, and Ag@LDH through simulations. (C–E) The confocal microscopy images of surface adsorption of fluorescent gaseous molecules experiment: (C) Ag wires, (D) Ag@ZIF-67, and (E) Ag@LDH. Inset: the fluorescence image and overlays of fluorescence and transmission images.⁴¹ Reproduced with permission from John Wiley and Sons, copyright 2019. (F) Illustration showing the adsorption process between molecules in exhaled gas and various substrates. (G) Modeling the variation in concentrations of GSPs@ZIF-8 and GSPs@H-ZIF-8 through simulations. (H) Simulations of alterations in the concentrations of GSPs@ZIF-8 and GSPs@H-ZIF-8. Inset: TEM images of GSPs@ZIF-8 and GSPs@H-ZIF-8.⁴⁰ Reproduced with permission from John Wiley and Sons, copyright 2022.

diverse range of pore sizes. This distinctive feature enables them to have superior gas permeability in comparison to ZIF-67. The reason behind this is their specific surface area and pore size distribution properties. In contrast, ZIF-67 has a denser structure with a narrower pore size distribution at the molecular level, which leads to a smaller diffusion coefficient. LDH nanocages have very low adsorption capacity for gaseous analytes, whereas Ag@LDH exhibits a concentration gradient that is comparable to that of Ag nanowires (Fig. 8B). This indicates that the target molecules are restricted to the surface of the Ag nanowires rather than the LDH medium. Further validation was carried out through experiments involving the adsorption of fluorescent molecules. The spatial locations of fluorescent molecules were examined using laser scanning confocal microscopy, for silver wires that were uncoated, coated with ZIF-67 and coated with LDH. Due to elastic collisions between molecules and substrates, the number of fluorescent

molecules observed on the exposed Ag nanowires was limited (Fig. 8C). The utilization of the ZIF-67 coating resulted in uniform dispersion of fluorescent molecules within the MOF layer. (Fig. 8D). The presence of LDH nanocages caused fluorescent molecules to be fixed closer to the surface of the silver wire. (Fig. 8E). The detection limit of aldehydes for the SERS sensor was 1.9 ppb.

Hollow ZIF-8 layers are capable of efficiently enriching gaseous molecules, similar to their solid ZIF-8 layers. After enrichment, the gas molecules can bind with functionalized molecules on the surface of PNPs, resulting in a strong and detectable reset signal. Wang and his team have developed a reliable SERS sensing platform strategy by coating GSPs with hollow structure ZIF-8 to detect exhaled VOCs (Fig. 8F).⁴⁰ Gas molecules are decelerated in their diffusion rate and accumulate within the cavity, while passing through the porous ZIF-8 (Fig. 8G). As a result, the efficiency of the chemical reaction for the target molecules is enhanced in the absence of kinetic energy. This leads to an increased number of molecules being trapped on the surface of the GSPs, resulting in the generation of robust Raman signals. (Fig. 8H). In contrast to solid MOFs, the active sites of modified molecules are free from non-reactive interfering molecules, thus allowing for more efficient target molecule capture. As a result of this, the lower LOD and reduced interference of non-target molecules in the SERS spectra make the results more trustworthy compared to GSPs@ZIF-8.

3.2 MOFs for selectively capturing target molecules

In the MOF-based SERS sensing platform, which is used for life and health detection, the MOF shell possesses a considerably large specific surface area,⁷⁸ uniform pore size,⁷⁹ and structural adaptability^{80,81} that make it ideal as a molecular sieve for PNPs/MOFs composite materials. The excellent crystallinity and pore size selectivity of MOFs allow target molecules to pass through, while preventing interference from larger size molecules.^{44,82} Additionally, the thickness of MOFs and the functional groups provided by organic ligands can affect selectivity.^{83,84} In real samples, identifying unknown components can be extremely challenging due to complex SERS signals caused by non-selective enrichment. However, the selective barrier provided by the porous MOF shell surrounding PNPs restricts the approach of analytes larger than the pore size, resulting in enhanced identification ability for analytes in complex samples within the SERS spectra. This improvement leads to higher accuracy and sensitivity in detecting target molecules.

VOCs serve as crucial biomarkers for the early diagnosis of diseases. However, due to their low concentration and high mobility, there are limited collisions between gas molecules and SERS substrates, which severely affect the detection sensitivity. However, the MOF shell plays an essential role in the selective detection of gaseous targets in complex VOC systems by pre-excluding them. Wang and his team used GSPs@ZIF-8 SERS substrates for selective detection of aldehydes, which are lung cancer biomarkers found in exhaled patient breath

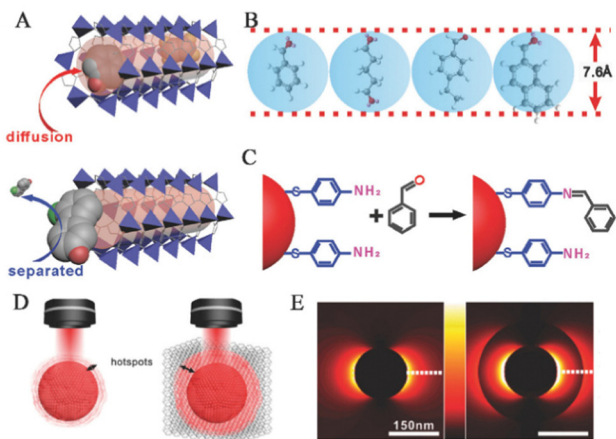


Fig. 9 Selectivity and synergistic effect based on MOFs. (A) The method of achieving selectivity for a particular analyte. (B) The largest size of the four primary analytes could permeate the holes of ZIF-8. (C) The chemical process is employed to bind aldehyde vapors covalently to the GSPs. (D) Schematic diagrams of LSPR hotspots located at the periphery of GSPs and GSPs@ZIF-8. (E) 2D-FDTD simulations of AuNPs and AuNPs@ZIF-8.¹⁴ Reproduced with permission from John Wiley and Sons, copyright 2018.

(Fig. 9A).¹⁴ Studies have shown that ZIF-8 can adsorb gaseous aromatic compounds such as benzene, xylene, toluene, and even 1,2,4-trimethylbenzene. In this system, benzaldehyde, glutaraldehyde, and 4-ethylbenzaldehyde can penetrate GSPs@ZIF-8, while 2-naphthaldehyde is excluded (Fig. 9B). Prolonged contact time between gaseous aldehyde molecules and SERS hotspots can help in producing Raman signals from gaseous aldehyde analytes.

In addition to physical adsorption, MOFs can selectively adsorb target molecules through chemical recognition. Yusuke and his team combined mesoporous plasma gold films with microporous homochiral metal-organic frameworks (HMOFs) to prepare graded porous hybrid membranes.⁸² They selectively detected pseudoephedrine (PE) in complex biological samples using surface-enhanced Raman spectroscopy. HMOF thin films are based on chiral ligands (alanine derivatives) as functional layers. In the presence of complex biological matrices, mixed-layered porous substrates provide control over molecular transport within pores and prevent blood protein penetration. The SERS substrate mentioned above utilizes surface-enhanced Raman spectroscopy technology to effectively detect and distinguish between two PE enantiomers with exceptional accuracy and sensitivity in even the most complex biological matrices, all without the need for preliminary separation.

3.3 Synergistic signal enhancement of MOF-based sensing platforms

Composite materials consisting of MOFs and PNPs offer benefits beyond selective adsorption and enrichment of target molecules. The synergistic effect between MOFs and PNPs enhances SERS detection of target analytes through surface plasmon resonance, which significantly amplifies the Raman cross section *via* the electromagnetic mechanism. However, this enhancement is limited to the surface of NPs due to the

rapid decay of the electromagnetic field near the metal/medium (usually air) interface.⁸⁵ By changing the relative dielectric constants of the metal and surrounding medium, the depth at which the electromagnetic field can penetrate can be altered.⁸⁶

Wang and his team utilized the finite-difference time-domain (FDTD) method to simulate the electric field distribution of GSPs and GSPs@ZIF-8.¹⁴ The simulation results demonstrated that the electromagnetic field intensity at the GSPs@ZIF-8 interface was stronger than that at the GSPs/air interface (Fig. 9D). This is attributed to the high dielectric constant of metal/medium (ZIF-8), which prevents radially attenuated electromagnetic fields.⁸⁵ Compared to bare GSPs, the GSPs@ZIF-8 structure provided a larger hotspot field (Fig. 9E), where both the bound and unbound analytes may be enhanced by the electromagnetic field. As a result, the Raman scattering intensity of the probe molecules on the GSPs@ZIF-8 core-shell structure under experimentation was roughly 1.5 times higher than that observed on the uncoated GSP substrate. These findings suggest that increasing the SERS signal strength through MOF-based SERS systems to increase electromagnetic field penetration depth is a universal strategy.

Recently, Jiang and his team created a pliable SERS substrate by embellishing AgNPs with ZIF-67 as the active constituent and adopting cotton fabric as the support framework.⁸⁷ When AgNPs come into direct contact with ZIF-67, charge transfer often occurs between them to balance the Fermi level and achieve equilibrium. Therefore, upon laser irradiation, polarization and charge transfer take place, leading to local electromagnetic field enhancement at the interface between AgNPs and ZIF-67, resulting in significantly improved SERS performance. Although there is limited research in this area currently, utilizing the synergistic effect of MOFs and metal NPs to develop efficient SERS substrates is a promising strategy.

3.4 MOFs for improving reproducibility and stability

Using PNPs for SERS detection poses a significant challenge due to their instability in complex environments.^{68,88} However, research has demonstrated that applying a protective layer on the surface of PNPs is an effective strategy for enhancing their stability. MOFs are ideal candidates for stabilizing layers, as they offer exceptional chemical and thermal stability, as well as mechanical robustness.^{89–91} The stability of MOFs can be evaluated based on three main aspects: thermal, humidity, and chemical stability. First, MOFs exhibit good thermal stability at high temperatures because of their strong intermolecular forces and covalent bonds between molecules. Some MOFs can even maintain their structural integrity at temperatures up to 500 °C.^{19,92} Second, humidity stability is closely related to the structure and composition of MOFs. The porous structure in MOFs can adsorb water molecules, which can cause instability and disintegration or loss of their structural integrity. However, some MOFs show good water stability because of their compact structure, synergistic effects between metal ions and organic ligands, and formation of internal hydrogen bond networks.^{93–95} Third, the chemical stability of MOFs is affected

by their crystal structure, chemical reactions, and acid–base properties. Metal ions used in some MOFs are susceptible to oxidation or reduction, which can damage the crystal structure and decrease performance. Additionally, certain organic ligands used in MOFs may undergo acid–base reactions, leading to MOF decomposition and deactivation. The acid–base stability is crucial when evaluating MOFs. In general, MOFs are stable under neutral or weakly acidic conditions, but they may lose structural integrity and performance under strong acidic or alkaline conditions. The acid–base stability is primarily determined by the MOFs' structure and composition, especially the intermolecular forces between metal ions and organic ligands, pore size, and coordination bond stability. For instance, ZIF-8 exhibits good stability under weakly acidic conditions below pH 6–7, but its structure can be destroyed under lower pH conditions.⁹⁶ On the other hand, MIL-101 shows higher stability under neutral or weakly acidic conditions and can tolerate a pH range of 2–12.⁴⁴ To enhance the stability of the MOFs, modifications can be made to the structure and composition, such as increasing the intermolecular forces between metal ions and organic ligands, adjusting pore size, and selecting organic ligands with greater chemical stability.

Wang and his team conducted an extensive study on the stability of the GSPs@ZIF-8 and GSPs@H-ZIF-8 SERS sensing platforms in complex gas environments.⁴⁰ In such environments, interfering molecules could potentially appear at the detection site, leading to unstable SERS sensor signals and reduced detection ability, which limits the practical application of these sensors. To ensure the stability of the substrates under these conditions, researchers injected mixed gases with interference molecules and 4-ethylbenzaldehyde in concentrations of 10 ppm into both substrates for continuous testing. Due to the remarkable adsorption ability of MOFs at the detection site, Raman signals for different molecules such as toluene and hydrocarbons were observed randomly on the GSPs@ZIF-8 substrate. However, the Raman signal of the hollow structure remained stable throughout the test. Both substrates underwent ten parallel experiments and the results showed that the spectral signal of the hollow structure had a higher repeatability and stability than that of its counterpart.

MIL-101 is a type of MOF that is highly regarded due to its impressive characteristics such as high surface area, large pore size, and exceptional stability in water and solvents. Recently, Li and his team created an extremely sensitive SERS substrate by embedding AuNPs into MIL-101.⁴⁴ The researchers then evaluated the stability and reproducibility of this substrate by measuring the SERS performance of both AuNPs/MIL-101 and AuNP colloids in different pH solutions containing benzidine. MIL-101 functions as a reliable host material by offering a closed space and adsorption field for analyte enrichment near the embedded metal surface. The SERS activity of AuNPs/MIL-101 remains stable within the pH range of 2–12, making it a highly desirable substrate for SERS detection. In comparison, the use of gold colloidal suspensions for detecting SERS can be limited because of the inherent instability caused by changes in the detection environment such as pH or ionic strength. This

instability can result in a loss of the SERS signal, and colloids may even precipitate from the solution. Additionally, due to the irregular aggregation of AuNP colloids, their Raman intensity varies significantly with pH. Overall, Li and his team's study demonstrated that the composite AuNPs/MIL-101 SERS substrate is not only highly sensitive but also possesses excellent stability and reproducibility.

To optimize MOF-based SERS sensing platforms, it is important to take into account the impact of the MOFs' crystal structure and chemical reactions on their stability. This will help ensure that the platform performs well and remains stable in applications such as life and health detection. In addition, it is crucial to select appropriate MOFs based on the specific application environment. This will ensure that the MOFs exhibit good stability and optimal performance under these conditions. By considering both the crystal structures and chemical properties of the MOFs, as well as the specific environmental factors of the intended applications, researchers can design more effective and reliable MOF-based SERS sensing platforms.

4. Application of MOF-based SERS sensing platforms in life and health detection

With their diverse microstructures and unique properties, MOFs have the potential to enhance SERS effects by enriching molecules and selectively absorbing them. MOF-based SERS sensing platforms can be integrated to enrich, capture, differentiate, and screen biological markers, allowing for early disease diagnosis (Table 1). Therefore, MOF-based SERS-active substrates provide unforeseen benefits and exceptional sensing capabilities for the detection of life and health, even under complicated background interferences such as human breath detection, bodily fluid analysis, and biological imaging of cells or tissues.

4.1 Human exhalation detection

Human exhaled breath contains a variety of VOCs, which are important endogenous biomolecules that provide rich information about human health. Research indicates that VOCs are closely related to many physiological processes associated with diseases.¹⁰⁹ For instance, the unique physiological processes and metabolism of lung cancer cells result in changes in metabolic pathways and abnormal expression of VOCs within cells.^{110–112} Compared to healthy individuals, lung cancer patients exhibit significant changes in the types and amounts of VOCs in their exhaled breath. Precise tracking of these essential VOCs can facilitate screening for multiple diseases.¹⁰⁹ SERS is a trace detection technology that can even extend to single-molecule detection.¹¹³ Its potential to non-invasively identify lung malignant tumors by detecting VOCs as biological markers could constitute a major advance in early cancer diagnosis. However, this application currently faces two primary limitations: (1) the majority of VOC biomarkers exhibit only minimal Raman scattering; (2) due to the rapid migration

Table 1 Applications of MOF-based SERS sensing platforms in life and health detection

Structures	MOF-based substrates	Synthesis strategies	Targets	Applications	Ref.
Core-shell	GSPs@ZIF-8	Bottle-around-ship	4-Ethylbenzaldehyde	VOCs	14
Yolk-shell	Ag@LDH	Bottle-around-ship	4-Ethylbenzaldehyde	VOCs	41
Yolk-shell	GSPs@H-ZIF-8	Bottle-around-ship	4-Ethylbenzaldehyde	VOCs	40
Core-shell	Ag@ZIF-67	Bottle-around-ship	Benzaldehyde	VOCs	97
Core-shell	GNRs-QDs@NU-901	Bottle-around-ship	Benzaldehyde	VOCs	98
Core-shell	AgNC@CA@ZIF-8	Bottle-around-ship	Benzaldehyde, 3-ethylbenzaldehyde	VOCs	99
Randomly embedded	AuNPs@MIL-101(Cr)	Ship-in-a-bottle	Toluene, 4-ethylbenzaldehyde	VOCs	100
Satellite	AgNPs@ZIF-67/g-C3N4	Ship-on-a-bottle	Benzaldehyde	VOCs	101
Satellite	AuNPs@Cu-TCPP	Ship-on-a-bottle	Carboxylesterase 1	Serum	102
Satellite	AgNPs@MIL-101(Fe)	Ship-on-a-bottle	Cholesterol	Serum	103
Randomly embedded	AuNP/AE-MIL-101(Cr)	Ship-in-a-bottle	Carboxylesterase 1	Serum	54
Satellite	AgNPs@homochiral MOF	Ship-on-a-bottle	D/L-cysteine, D/L-asparagine	—	57
Core-shell	Ag@Ni-MOF-1	Bottle around ship	Cys	Microdialysate	104
Satellite	IRMOF-3@AuTPs	Ship-on-a-bottle	NT-proBNP	Serum	105
Randomly embedded	AuNPs@MIL-101	Ship-in-a-bottle	Glucose, lactate	Microdialysate	55
Satellite	AuNPs/Cu-TCPP(Fe)	Ship-on-a-bottle	Glucose	Saliva	62
Satellite	AgNPs/MIL-101(Fe)	Ship-on-a-bottle	DA	Urine	59
Randomly embedded	AuNPs/MIL-101	Ship-in-a-bottle	Alpha-fetoprotein	Serum	44
Satellite	AuNPs/MOF	Ship-on-a-bottle	Transferrin	Serum	66
Core-shell	Au@Cu ₃ (BTC) ₂	Bottle-around-ship	Cell	Bioimaging	106
Core-shell	AuNSs@ZIF-8	Bottle-around-ship	Cell	Bioimaging	107
Core-shell	Au@Ag nanorod@ZIF-8	Bottle-around-ship	Cell	Bioimaging	108

of gaseous molecules, they are minimally adsorbed on solid substrates. Integration of MOF-based SERS sensing platforms enables the enrichment, capture, distinction, and screening of biological markers in exhaled breath, thus achieving an early diagnosis of multiple diseases.

Wang and his team have proposed a method to enhance the adsorption ability of gaseous molecules on SERS sensing platforms by using GSPs@ZIF-8 SERS substrates to detect VOC biomarkers in the exhaled breath of lung cancer patients, achieving a highly sensitive strategy for early cancer diagnosis (Fig. 10A).¹⁴ ZIF-8 plays multiple roles in the core-shell SERS

substrates, including: (1) modifying the transport pathways and processes of gas molecules through the porous structure of the ZIF-8 shell, overcoming the obstacle of gas molecule adsorption on solid matrices; (2) significantly prolonging the contact time between gas molecules and the porous substrate by means of the ZIF-8 shell layer of GSPs, achieving the enrichment of target molecules; (3) playing a crucial part in selective detection, particularly in precluding complex VOC targets within the gas mixture, thus enabling selective detection of target molecules; and (4) safeguarding GSPs from external environmental interference by virtue of its stable framework structure, thereby enhancing the accuracy and reliability of SERS detection. By capturing gaseous aldehydes and reacting them with 4-ATP pre-anchored onto GSPs, the detection limit was 10 ppb, demonstrating great potential for early diagnosis of lung cancer. The GSPs@ZIF-8 structure has the ability to selectively track gaseous cancer biomarkers in mixed gases, demonstrating strong practical potential in actual applications and further enabling the non-invasive identification of lung malignancies.

Due to the characteristics of gas flow and porosity, the reproducibility and accuracy of SERS sensing platforms are difficult to achieve, but clinical detection of molecular markers using VOC sensors requires essential reproducibility and accuracy. To advance the practical clinical application of SERS sensors, researchers converted them into barcodes. For example, Wang and his team designed a hollow Co-Ni Ag@LDH to enhance the adsorption and capture of gaseous molecules (Fig. 10B).⁴¹ In contrast to Ag@ZIF-67, the target analyte had higher reaction or absorption efficiency at the active SERS site. Therefore, the Ag@LDH SERS sensor exhibited an LOD of 1.9 ppb, which was ten times lower than that of Ag@ZIF-67. By integrating the R, G, and B values of the Raman intensity image, the researchers obtained a unique barcode that represents the aldehyde concentration. Electronic devices such as smartphones and handheld scanners can easily scan and

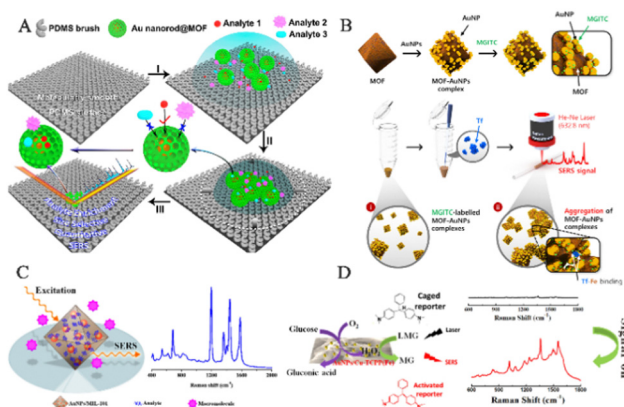


Fig. 10 Schematic diagram of MOF-based SERS sensing platforms used in human exhaled breath. (A) Schematic diagram of VOC detection via SERS spectroscopy.¹⁴ Reproduced with permission from John Wiley and Sons, copyright 2018. (B) Schematic diagram of a SERS sensing platform for VOC detection.⁴¹ Reproduced with permission from John Wiley and Sons, copyright 2019. (C) Schematic diagram of breath analysis using an Ag@ZIF-67-based tubular SERS sensor.⁹⁷ Reproduced with permission from American Chemical Society, copyright 2022. (D) Schematic diagram of the mask sensing device for the breath test.⁴⁰ Reproduced with permission from John Wiley and Sons, copyright 2022.

decode these barcodes. The findings of this research indicate the feasible capability of utilizing this sensor as a device to identify and screen biomarkers. Similarly, oxygenated metabolites such as aldehydes and ketones are linked to oxidative stress and inflammation,^{114,115} which may contribute to the development of cancer.¹¹⁶ Wang and his team have developed a tube-shaped SERS sensor with 4-ATP-modified Ag@ZIF-67 to identify various types of aldehyde–ketone VOCs and exhaled breath samples (Fig. 10C).⁹⁷ We conducted extensive studies on the SERS spectra of respiratory samples from GC patients and healthy volunteers and transformed them into barcodes for easy application in clinical settings. The findings demonstrate that the tube-shaped SERS sensor has high sensitivity and specificity in diagnosing gastric cancer, thereby offering an alternative solution for early cancer screening as it is non-invasive, quick and user-friendly.

Recently, Wang and his team demonstrated the selective detection of biomarkers in exhaled breath samples using a GSPs@H-ZIF-8 substrate, while minimizing the effect of interfering gas molecules on Raman spectra (Fig. 10D).⁴⁰ The hollow-structured MOF shell of GSPs@H-ZIF-8 does not trap interfering gas molecules within SERS hotspots, thus preventing reduced LOD and interference signals due to occupancy of sensing sites by interfering molecules. Consequently, GSPs@H-ZIF-8 substrates exhibit LODs for aldehyde molecules that are an order of magnitude lower than those of GSPs@ZIF-8 in complex environments. The substrate was then integrated into a respiratory valve to form a mask-type sensor. Raman spectra were acquired after 20 minutes of wearing, and PC-LDA was used to classify the results with an accuracy of 60%. These findings demonstrate the enormous potential of this sensor in the early detection of lung cancer.

The use of MOFs in the yolk structure of the SERS substrate offers several advantages. First, the MOF shell and cavity structure increase the interaction between the target molecules and the SERS substrate, thereby achieving enrichment of the target molecules. This is because the MOF structure effectively prolongs the contact time between the SERS substrate and target molecules. Second, the uniformly sized cavities with molecular sieving effects confer size-selective properties on the substrate, enabling selective detection of the target molecules. This means that the SERS substrate can selectively detect specific molecules on the basis of their size. Finally, the stable framework structure of the MOFs protects the plasmonic nanoparticles (such as Ag nanowires and GSPs) from external influences, improving the accuracy and reliability of SERS detection. Overall, incorporating MOFs into the yolk structure of the SERS substrate enhances its performance and provides several benefits for SERS detection.

4.2 Human body fluid detection

The MOF-based SERS sensing platform has the potential for detecting not only human exhaled breath but also low-concentration biomarkers in bodily fluids such as blood, urine, and saliva, allowing for early diagnosis of various diseases. However, bodily fluid detection presents a more complex

biological background compared to exhaled breath detection, which poses challenges to the development of MOF-based SERS sensing platforms for life and health monitoring. In order to overcome these challenges and better detect biomarkers in complex bodily fluid environments, Yang and his team created an integrated SERS platform called AEF-SERS. This platform has analyte enrichment and filtering capabilities, as well as powerful quantitative ability, high sensitivity, and enhanced analyte identification (Fig. 11A).¹¹⁷ To achieve this, they grew MOFs on gold nanorods to prevent the formation of the hottest spots between gold nanorods, resulting in strong quantitative ability. The porous MOF shell also acts as an analyte filter, preventing large analytes from approaching the inner gold nanorods, simplifying the SERS spectrum and enhancing analyte identification. The team successfully demonstrated selective detection of nano-level concentrations of 4-nitrobenzene thiol (4-NBT) in whole blood. It is envisioned that by adjusting the pore size of the MOF shell and analyzing disease biomarkers in biological fluids like blood and urine, the AEF-SERS system has broad application prospects for health monitoring.

In the application of SERS biosensors, there are two major prerequisites to achieve successful enhancement of SERS signals. Firstly, the SERS substrate should have a high capacity to adsorb reporter molecules and be positioned in close proximity to the outer surface of the PNPs. Secondly, it is important to create numerous plasmonic nanogaps at the active interface between neighboring PNPs. Therefore, the reporter molecules should be located in the vicinity of the plasmonic active site of the SERS-active substrate in order to optimize the enhancement of SERS signals. To meet these requirements, Choo and his team developed a new type of SERS-active AuNPs/MOFs complex by attaching citrate-capped AuNPs to the surface of

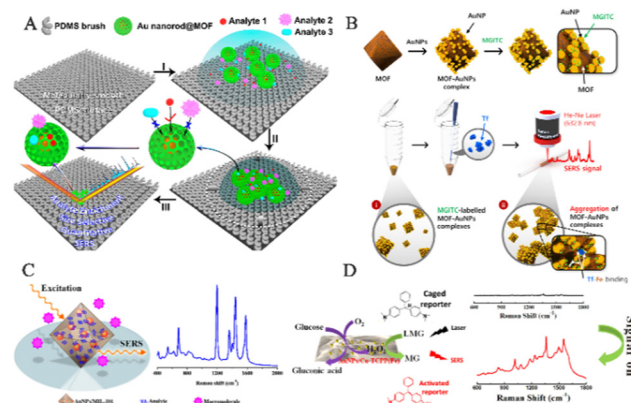


Fig. 11 Schematic diagram of MOF-based SERS sensing platforms employed in human body fluid detection. (A) Schematic diagram of the operational mechanism of the AEF-SERS platform.¹¹⁷ Reproduced with permission from American Chemical Society, copyright 2020. (B) Schematic diagram of the fabrication of SERS-active AuNPs/MOF complexes.⁶⁶ Reproduced with permission from John Wiley and Sons, copyright 2021. (C) Schematic diagram of alpha-fetoprotein detection based on SERS.⁴⁴ Reproduced with permission from American Chemical Society, copyright 2014. (D) Schematic illustration of SERS-based glucose sensing.⁶² Reproduced with permission from American Chemical Society, copyright 2020.

the amine-functionalized MOFs (Fig. 11B).⁶⁶ When the AuNPs/MOFs complex is mixed with Raman reporter molecules, the pores in the MOFs can adsorb a large number of reporter molecules, promoting the reporter molecules to approach the AuNPs on the solid MOF matrix. Thus, many reporter molecules are captured near the SERS-active “hotspots”, significantly enhancing their SERS signals. In the presence of transferrin, the transferrin-Fe(III) bond leads to the formation of an aggregated AuNPs/MOF network, further increasing the SERS signal intensity of AuNPs/MOFs. The SERS-based transferrin analysis method provides a new SERS platform for accurately measuring transferrin TIBC in human blood samples.

The MOF-based SERS platform not only enables the direct detection of biomolecules in bodily fluids but also serves as an immunosorbent assay for selective and quantitative biomarker detection. The MOFs coating enhances analyte enrichment and SERS hotspots. Li and his team developed a highly sensitive SERS detection method using AuNPs embedded in MIL-101 (Fig. 11C).⁴⁴ The synthesis method involved the impregnation of a solution containing chloroauric acid and sodium citrate, followed by their *in situ* growth and encapsulation within the host matrix of MIL-101. The resulting AuNPs/MIL-101 nanocomposite offers both local surface plasmon resonance properties of AuNPs and the high adsorption capacity of MOF substrates, producing a highly sensitive SERS substrate that concentrates analytes at the SERS-active metal surface electromagnetic field. This new SERS substrate is suitable for clinical samples. The team established a SERS-ELISA-based method to quantitatively analyze alpha-fetoprotein in human serum, with a linear range of 1.0–130.0 ng mL⁻¹ and a correlation coefficient of 0.9938. Tamer and his team employed antibody-functionalized magnetic MOFs as capture probes for urine samples, developing a microfluidic chip-driven immunoassay to detect the human chorionic gonadotropin (hCG) protein banned by the World Anti-Doping Agency.¹¹⁸ With spatial restriction and size selection advantages, the coating of MOFs can be combined with catalysts to promote difficult-to-perform chemical reactions and exclude potential interference with biomarker recognition. MOFs play a crucial role in the randomly embedded structure of the SERS substrate, serving multiple functions such as (1) retaining the high-level nanoporous structure of the network by embedding PNPs within MOF frameworks, allowing for the dispersion and isolation of PNPs/MOFs that can enrich analytes for analysis; (2) locating the SERS active sites of PNPs on the grid structure, which promotes close proximity to target molecules within pores and enhances detection sensitivity; and (3) maintaining water stability of MOFs to ensure the stability of PNPs/MOFs composite materials in aqueous solutions, thereby improving the reproducibility of SERS detection. Yang and his team synthesized a multifunctional AuNPs/Cu-TCPP(Fe) composite material by modifying AuNPs on 2D metalloporphyrin MOFs (Fig. 11D).⁶² Cu-TCPP(Fe) nanosheet has peroxidase-like activity, while AuNPs have Gox mimetic activity, inducing cascade catalytic reactions converting glucose to H₂O₂ and then

oxidizing non-Raman-active LMG to Raman-active MG *via* AuNP catalysis. This non-enzyme SERS detection method based on AuNPs/Cu-TCPP(Fe) nanosheets was used for glucose detection in saliva, providing a new approach to designing nano-enzyme-based SERS protocols for biomarker analysis.

4.3 Bioimaging

SERS bioimaging is a highly sensitive imaging technique that uses the SERS effect of PNPs to amplify the Raman signal of samples. In this process, MOF-based SERS probes are modified with chemical reaction groups or affinity labels, allowing for selective binding to the surface of biomolecules. Compared to fluorescence probes, MOF-based SERS probes have many advantages: first, they can detect molecules at very low concentrations because PNPs significantly enhance the Raman signal; second, they are less susceptible to photobleaching and thus more photostable than fluorescent probes; third, through unique fingerprint vibrational spectra, MOF-based SERS probes can identify the unique structure of target molecules; and finally, MOF-based SERS probes have low interference in aqueous solutions, avoiding misjudgments due to solvent effects.¹¹⁹ These advantages have made MOF-based SERS probes widely used and rapidly developed in bio-imaging. Their excellent biocompatibility and superior SERS performance enable real-time tracking of tumor cells and SERS bio-imaging. The MOF-based SERS sensing platform has important potential in bioimaging and will become a key technology in the field of life and health detection.

Therefore, He and his team used chemically encapsulated Raman reporters to prepare a diagnostic core–shell Au@Cu₃(BTC)₂ composite material for bioimaging.¹⁰⁶ A controllable growth approach was used to prepare Au@Cu₃(BTC)₂ composite material, which involved depositing a Cu₃(BTC)₂ shell on a gold core that had been modified with the Raman reporter molecule 4-mercaptopbenzoic acid (4-MBA). In contrast to prior core–shell metal@MOFs, this new approach involves the participation of Raman reporter molecules featuring distinguishable Raman signals in connecting both the AuNPs and MOFs, thus eliminating the need for extra modification of Raman reporter molecules and streamlining the synthesis procedure.

However, the inherent water instability of MOFs remains challenging and unresolved. Therefore, Carrillo-Carrion and his team synthesized core–shell gold nanostars/ZIF-8 (AuNSs@ZIF-8) nanocomposites for precise release of thermoplastic-driven active molecules encapsulated in live cells, which can be observed by SERS imaging before and after intracellular release (Fig. 12A).¹⁰⁷ MOF-based SERS probes can not only perform SERS imaging of cells but also tissue imaging. Jiang and his team reported the successful creation of Au@Ag nanorod@ZIF-8 for accurate cancer cell imaging through the application of SERS (Fig. 12B).¹⁰⁸ The composite material is composed of SERS nano-labels and ZIF-8 coatings. The intermediate layer is a SERS nano-label consisting of Au@Ag nanorods and reporter molecules. In summary, the presence of the ZIF-8 outer coating isolates external interference with the SERS

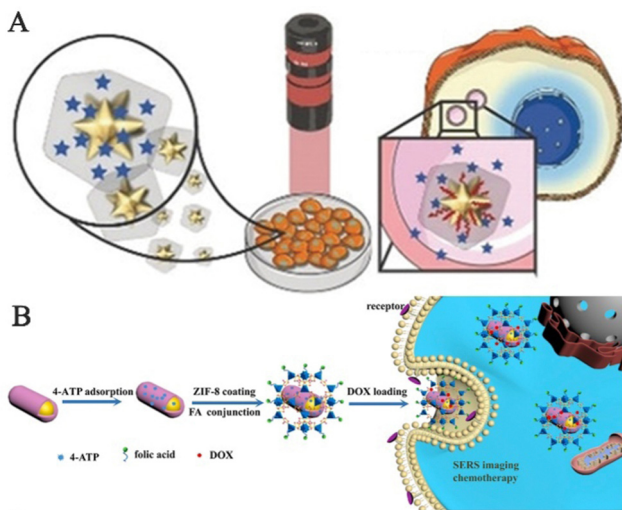


Fig. 12 Schematic diagram of MOF-based SERS sensing platforms employed in bioimaging. (A) Schematic diagram of intracellular SERS imaging of Au nanostar@ZIF-8.¹⁰⁷ Reproduced with permission from John Wiley and Sons, copyright 2019. (B) Schematic diagram of the synthetic route and application instructions of Au@Ag nanorod@ZIF-8.¹⁰⁸ Reproduced with permission from Elsevier, copyright 2019.

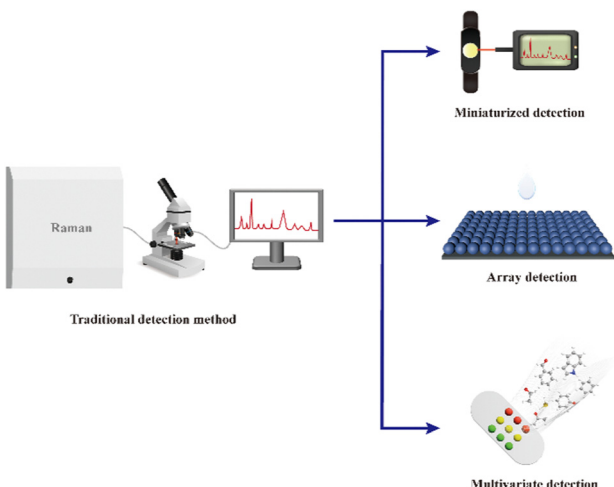


Fig. 13 The future development direction of the MOF-based SERS sensor platforms for life and health detection.

nano-label, making it easy to load and modify, which makes the NPs superior to other probes in biochemical applications. The probe was then utilized for SERS imaging of low-cytotoxicity human colon cancer cells and tumor tissues.

5. Conclusions and perspectives

The combination of MOFs and SERS technology is a prevailing trend in the field of analysis and detection. There are two primary reasons for this development. First, the progress of analysis and detection technology is heavily based on the advancement of materials science. The construction and design

of SERS sensors for life sciences requires support from materials science, and the successful production of MOF-based SERS substrates has enabled the manufacturing of high-performance SERS sensing platforms. As a result, this paper presents four strategies for producing MOF-based SERS substrates for analysis and detection (bottle-around-ship strategy, ship-in-a-bottle strategy, ship-on-a-bottle strategy, and one-pot strategy). Different preparation methods yield distinct structures of MOF-based SERS substrates (core–shell, yolk–shell, satellite, and random embedding structures). Second, SERS technology itself has shortcomings that require innovation and advancement when applied to life and health detection. The application of emerging MOFs to produce novel MOF-based SERS sensing platforms can increase the development of SERS technology and offers numerous advantages over other combined strategies. Therefore, this paper elucidates the functions of MOFs in MOF-based SERS sensing platforms, which provides opportunities for analyzing and detecting trace biological markers. The main roles of MOFs in MOF-based SERS platforms include concentrating trace biological markers, enhancing detection sensitivity, and selectively and specifically identifying target molecules, while eliminating other interfering molecules, acting as a protective shield to maintain their biocompatibility under complex conditions with robust stability and reproducibility, and synergistically interacting with plasmas to enhance SERS detection performance. Finally, this paper summarizes the potential applications of MOF-based SERS sensing platforms in life and health detection applications.

Despite the rapid development of MOF-based SERS substrates, which have opened up new possibilities for detecting trace biological markers using SERS technology, they still face several challenges. First, while many studies have reported successful preparation of MOF-based SERS substrates, extensive research is needed to design and synthesize MOF-based SERS substrates that are easy to make, stable, reproducible, and have high enhancement factors. The large-scale preparation of MOF-based SERS substrates in a single form is also challenging, as it can impact the uniformity, accuracy, and reproducibility of SERS signals in life and health detection. Second, the introduction of MOFs can reduce interference from non-target molecules in complex environments, thereby enhancing the accuracy of SERS sensing platforms for trace target biomolecules in complex systems. Therefore, further exploration of new MOFs with high selectivity for identifying target biomolecules in complex systems and improving the anti-interference capabilities of MOF-based SERS substrates for analysis and detection applications is necessary. However, achieving the fingerprint identification of individual molecules in biological analysis and detection remains difficult. Third, limited research exists on MOF-based SERS substrates solely used for detecting trace biological markers mainly due to the contribution of MOFs to SERS enhancement not being extensively studied and explained. Hence, these issues require further investigation, and the enhancement mechanism of MOF-based SERS substrates needs thorough research to meet

the demands of MOF-based SERS sensing platforms in life and health detection applications.

Despite facing numerous difficulties and challenges, MOF-based SERS sensing platforms offer unique advantages over traditional SERS platforms. These materials form a strong foundation for achieving high-performance SERS detection, particularly for detecting trace amounts of biomarkers. As a result, MOF-based SERS sensing platforms show great promise in the field of life and health detection (Fig. 13). Moving forward, research in this area can focus on various aspects, such as designing and preparing miniaturized MOF-based SERS substrates that can be combined with portable Raman spectrometers to enable chip-based detection and real-time monitoring of multiple diseases. Additionally, 3D printing technology can be utilized to fabricate array-structured MOF-based SERS substrates, allowing for precise control over parameters such as pore morphology, size, and arrangement within the substrate, thereby enhancing the SERS signal. MOFs also provide an opportunity to achieve precise control over pore sizes and shapes by adjusting organic ligands and metal ions within frameworks. This can improve the accuracy and reproducibility of analysis results, while eliminating interference from complex systems. Finally, MOF-based SERS sensing platforms can be designed and constructed with multi-functional and diversified detection capabilities by modifying different functional groups on their surfaces. In doing so, they can facilitate the adsorption of biomarker molecules from various diseases, leading to accurate and rapid diagnosis of different types of diseases. Deep learning-based component identification for the Raman spectra of mixtures holds great promise for achieving accurate and efficient multi-target detection.¹²⁰ By combining this approach with SERS platforms based on MOFs, it becomes possible to detect multiple targets in complex mixtures with improved precision. Integrating deep learning algorithms into Raman spectroscopic analysis obtained from MOF-based SERS platforms has the potential to significantly enhance the speed and accuracy of multi-target detection and identification. With further advancements in MOFs and SERS, the prospects of MOF-based SERS sensing platforms in life and health detection are remarkably promising.

Author contributions

This manuscript was written through the contributions of all authors. All authors gave approval for the final version.

Conflicts of interest

There are no conflicts to declare.

Acknowledgements

This work was financially supported by the National Natural Science Foundation of China (21925405) and the National Key Research and Development Program of China (2021YFFD1700300).

References

- 1 L. Huang, H. Sun, L. Sun, K. Shi, Y. Chen, X. Ren, Y. Ge, D. Jiang, X. Liu, W. Knoll, Q. Zhang and Y. Wang, Rapid, label-free histopathological diagnosis of liver cancer based on Raman spectroscopy and deep learning, *Nat. Commun.*, 2023, **14**, 48.
- 2 M. Rudin and R. Weissleder, Molecular imaging in drug discovery and development, *Nat. Rev. Drug Discovery*, 2003, **2**, 123–131.
- 3 R. Weissleder, Molecular Imaging in Cancer, *Science*, 2006, **312**, 1168–1171.
- 4 N. M. Ralbovsky and I. K. Lednev, Towards development of a novel universal medical diagnostic method: Raman spectroscopy and machine learning, *Chem. Soc. Rev.*, 2020, **49**, 7428–7453.
- 5 M. Chen, X. He, K. Wang, D. He, X. Yang and H. Shi, Inorganic fluorescent nanoprobes for cellular and subcellular imaging, *TrAC, Trends Anal. Chem.*, 2014, **58**, 120–129.
- 6 X. Huang, J. Song, B. C. Yung, X. Huang, Y. Xiong and X. Chen, Ratiometric optical nanoprobes enable accurate molecular detection and imaging, *Chem. Soc. Rev.*, 2018, **47**, 2873–2920.
- 7 D. Cialla-May, X. S. Zheng, K. Weber and J. Popp, Recent progress in surface-enhanced Raman spectroscopy for biological and biomedical applications: from cells to clinics, *Chem. Soc. Rev.*, 2017, **46**, 3945–3961.
- 8 Z. Chen, G. Li and Z. Zhang, Miniaturized Thermal-Assisted Purge-and-Trap Technique Coupling with Surface-Enhanced Raman Scattering for Trace Analysis of Complex Samples, *Anal. Chem.*, 2017, **89**, 9593–9600.
- 9 M. F. Cardinal, E. Vander Ende, R. A. Hackler, M. O. McAnally, P. C. Stair, G. C. Schatz and R. P. Van Duyne, Expanding applications of SERS through versatile nanomaterials engineering, *Chem. Soc. Rev.*, 2017, **46**, 3886–3903.
- 10 S. Laing, L. E. Jamieson, K. Faulds and D. Graham, Surface-enhanced Raman spectroscopy for in vivo biosensing, *Nat. Rev. Chem.*, 2017, **1**, 0060.
- 11 I. Zare, M. T. Yaraki, G. Speranza, A. H. Najafabadi, A. Shourangiz-Haghghi, A. B. Nik, B. B. Manshian, C. Saraiva, S. J. Soenen, M. J. Kogan, J. W. Lee, N. V. Apollo, L. Bernardino, E. Araya, D. Mayer, G. Mao and M. R. Hamblin, Gold nanostructures: synthesis, properties, and neurological applications, *Chem. Soc. Rev.*, 2022, **51**, 2601–2680.
- 12 S.-Y. Ding, E.-M. You, Z.-Q. Tian and M. Moskovits, Electromagnetic theories of surface-enhanced Raman spectroscopy, *Chem. Soc. Rev.*, 2017, **46**, 4042–4076.
- 13 H. Lai, F. Xu, Y. Zhang and L. Wang, Recent progress on graphene-based substrates for surface-enhanced Raman scattering applications, *J. Mater. Chem. B*, 2018, **6**, 4008–4028.
- 14 X. Qiao, B. Su, C. Liu, Q. Song, D. Luo, G. Mo and T. Wang, Selective Surface Enhanced Raman Scattering for Quantitative Detection of Lung Cancer Biomarkers in Superparticle@MOF Structure, *Adv. Mater.*, 2018, **30**, 1702275.

15 G. Demirel, H. Usta, M. Yilmaz, M. Celik, H. A. Alidagi and F. Buyukserin, Surface-enhanced Raman spectroscopy (SERS): an adventure from plasmonic metals to organic semiconductors as SERS platforms, *J. Mater. Chem. C*, 2018, **6**, 5314–5335.

16 D. Cialla-May, X. S. Zheng, K. Weber and J. Popp, Recent progress in surface-enhanced Raman spectroscopy for biological and biomedical applications: from cells to clinics, *Chem. Soc. Rev.*, 2017, **46**, 3945–3961.

17 O. M. Yaghi, M. O'Keeffe, N. W. Ockwig, H. K. Chae, M. Eddaoudi and J. Kim, Reticular synthesis and the design of new materials, *Nature*, 2003, **423**, 705–714.

18 C. Huang, A. Li, X. Chen and T. Wang, Understanding the Role of Metal–Organic Frameworks in Surface-Enhanced Raman Scattering Application, *Small*, 2020, **16**, 2004802.

19 H. Furukawa, K. E. Cordova, M. O'Keeffe and O. M. Yaghi, The Chemistry and Applications of Metal–Organic Frameworks, *Science*, 2013, **341**, 1230444.

20 X. Deng, S. Liang, X. Cai, S. Huang, Z. Cheng, Y. Shi, M. Pang, P. A. Ma and J. Lin, Yolk–Shell Structured Au Nanostar@Metal–Organic Framework for Synergistic Chemo-photothermal Therapy in the Second Near-Infrared Window, *Nano Lett.*, 2019, **19**, 6772–6780.

21 Y. Cui, J. Zhang, H. He and G. Qian, Photonic functional metal–organic frameworks, *Chem. Soc. Rev.*, 2018, **47**, 5740–5785.

22 A. Campion and P. Kambhampati, Surface-enhanced Raman scattering, *Chem. Soc. Rev.*, 1998, **27**, 241–250.

23 C. Huang, C. Liu, X. Chen, Z. Xue, K. Liu, X. Qiao, X. Li, Z. Lu, L. Zhang, Z. Lin and T. Wang, A Metal–Organic Framework Nanosheet-Assembled Frame Film with High Permeability and Stability, *Adv. Sci.*, 2020, **7**, 1903180.

24 J. Yang and Y.-W. Yang, Metal–Organic Frameworks for Biomedical Applications, *Small*, 2020, **16**, 1906846.

25 L. J. Murray, M. Dincă and J. R. Long, Hydrogen storage in metal–organic frameworks, *Chem. Soc. Rev.*, 2009, **38**, 1294–1314.

26 T. D. Bennett, A. K. Cheetham, A. H. Fuchs and F.-X. Coudert, Interplay between defects, disorder and flexibility in metal–organic frameworks, *Nat. Chem.*, 2017, **9**, 11–16.

27 Z. Chang, D.-H. Yang, J. Xu, T.-L. Hu and X.-H. Bu, Flexible Metal–Organic Frameworks: Recent Advances and Potential Applications, *Adv. Mater.*, 2015, **27**, 5432–5441.

28 L. Jiao, J. Y. R. Seow, W. S. Skinner, Z. U. Wang and H.-L. Jiang, Metal–organic frameworks: Structures and functional applications, *Mater. Today*, 2019, **27**, 43–68.

29 T. Simon-Yarza, A. Mielcarek, P. Couvreur and C. Serre, Nanoparticles of Metal–Organic Frameworks: On the Road to In Vivo Efficacy in Biomedicine, *Adv. Mater.*, 2018, **30**, 1707365.

30 Q.-L. Zhu and Q. Xu, Metal–organic framework composites, *Chem. Soc. Rev.*, 2014, **43**, 5468–5512.

31 C. R. Kim, T. Uemura and S. Kitagawa, Inorganic nanoparticles in porous coordination polymers, *Chem. Soc. Rev.*, 2016, **45**, 3828–3845.

32 Y. Liu and Z. Tang, Multifunctional Nanoparticle@MOF Core–Shell Nanostructures, *Adv. Mater.*, 2013, **25**, 5819–5825.

33 A. Dhakshinamoorthy and H. Garcia, Catalysis by metal nanoparticles embedded on metal–organic frameworks, *Chem. Soc. Rev.*, 2012, **41**, 5262–5284.

34 H. R. Moon, D.-W. Lim and M. P. Suh, Fabrication of metal nanoparticles in metal–organic frameworks, *Chem. Soc. Rev.*, 2013, **42**, 1807–1824.

35 D. Men, S. Feng, G. Liu, L. Hang and T. Zhang, A Sensitive “Optical Nose” for Detection of Volatile Organic Molecules Based on Au@MOFs Nanoparticle Arrays through Surface-Enhanced Raman Scattering, *Part. Part. Syst. Charact.*, 2020, **37**, 1900452.

36 L. E. Kreno, N. G. Greeneltch, O. K. Farha, J. T. Hupp and R. P. Van Duyne, SERS of molecules that do not adsorb on Ag surfaces: a metal–organic framework-based functionalization strategy, *Analyst*, 2014, **139**, 4073–4080.

37 J. H. Fu, Z. Zhong, D. Xie, Y. J. Guo, D. X. Kong, Z. X. Zhao, Z. X. Zhao and M. Li, SERS-Active MIL-100(Fe) Sensory Array for Ultrasensitive and Multiplex Detection of VOCs, *Angew. Chem., Int. Ed.*, 2020, **59**, 20489–20498.

38 Q.-K. Fan, T.-Z. Liu, H.-S. Li, S.-M. Zhang, K. Liu and C.-B. Gao, Gold/oxide heterostructured nanoparticles for enhanced SERS sensitivity and reproducibility, *Rare Met.*, 2019, **39**, 834–840.

39 Q.-Q. Chen, R.-N. Hou, Y.-Z. Zhu, X.-T. Wang, H. Zhang, Y.-J. Zhang, L. Zhang, Z.-Q. Tian and J.-F. Li, Au@ZIF-8 Core–Shell Nanoparticles as a SERS Substrate for Volatile Organic Compound Gas Detection, *Anal. Chem.*, 2021, **93**, 7188–7195.

40 A. Li, X. Qiao, K. Liu, W. Bai and T. Wang, Hollow Metal Organic Framework Improves the Sensitivity and Anti-Interference of the Detection of Exhaled Volatile Organic Compounds, *Adv. Funct. Mater.*, 2022, **32**, 2202805.

41 X. Qiao, X. Chen, C. Huang, A. Li, X. Li, Z. Lu and T. Wang, Detection of Exhaled Volatile Organic Compounds Improved by Hollow Nanocages of Layered Double Hydroxide on Ag Nanowires, *Angew. Chem., Int. Ed.*, 2019, **58**, 16523–16527.

42 Q. Wang, Z. Shi, Z. Wang, Y. Zhao, J. Li, H. Hu, Y. Bai, Z. Xu, H. Zhangsun and L. Wang, Rapid simultaneous adsorption and SERS detection of acid orange II using versatile gold nanoparticles decorated NH₂-MIL-101(Cr), *Anal. Chim. Acta*, 2020, **1129**, 126–135.

43 D. Sun, G. Qi, K. Ma, X. Qu, W. Xu, S. Xu and Y. Jin, Tumor Microenvironment-Activated Degradable Multifunctional Nanoreactor for Synergistic Cancer Therapy and Glucose SERS Feedback, *iScience*, 2020, **23**, 101274.

44 Y. Hu, J. Liao, D. Wang and G. Li, Fabrication of Gold Nanoparticle-Embedded Metal–Organic Framework for Highly Sensitive Surface-Enhanced Raman Scattering Detection, *Anal. Chem.*, 2014, **86**, 3955–3963.

45 X. Cao, S. Hong, Z. Jiang, Y. She, S. Wang, C. Zhang, H. Li, F. Jin, M. Jin and J. Wang, SERS-active metal–organic frameworks with embedded gold nanoparticles, *Analyst*, 2017, **142**, 2640–2647.

46 J. H. Fu, Z. Zhong, D. Xie, Y. J. Guo, D. X. Kong, Z. X. Zhao, Z. X. Zhao and M. Li, SERS-Active MIL-100(Fe) Sensory Array for Ultrasensitive and Multiplex Detection of VOCs, *Angew. Chem., Int. Ed.*, 2020, **59**, 20489–20498.

47 T. Lin, H. Wang, C. Cui, W. Liu and G. Li, Recent Advances on Confining Noble Metal Nanoparticles Inside Metal–Organic Frameworks for Hydrogenation Reactions, *Chem. Res. Chin. Univ.*, 2022, **38**, 1309–1323.

48 G. Lu, S. Li, Z. Guo, O. K. Farha, B. G. Hauser, X. Qi, Y. Wang, X. Wang, S. Han, X. Liu, J. S. DuChene, H. Zhang, Q. Zhang, X. Chen, J. Ma, S. C. Loo, W. D. Wei, Y. Yang, J. T. Hupp and F. Huo, Imparting functionality to a metal–organic framework material by controlled nanoparticle encapsulation, *Nat. Chem.*, 2012, **4**, 310–316.

49 X. Deng, L. Yang, H. Huang, Y. Yang, S. Feng, M. Zeng, Q. Li and D. Xu, Shape-Defined Hollow Structural Co-MOF-74 and Metal Nanoparticles@Co-MOF-74 Composite through a Transformation Strategy for Enhanced Photocatalysis Performance, *Small*, 2019, **15**, 1902287.

50 Q. Yang, Q. Xu and H. L. Jiang, Metal–organic frameworks meet metal nanoparticles: synergistic effect for enhanced catalysis, *Chem. Soc. Rev.*, 2017, **46**, 4774–4808.

51 B. Li, J.-G. Ma and P. Cheng, Integration of Metal Nanoparticles into Metal–Organic Frameworks for Composite Catalysts: Design and Synthetic Strategy, *Small*, 2019, **15**, 1804849.

52 P. Hu, J. V. Morabito and C.-K. Tsung, Core–Shell Catalysts of Metal Nanoparticle Core and Metal–Organic Framework Shell, *ACS Catal.*, 2014, **4**, 4409–4419.

53 X. Cao, S. Hong, Z. Jiang, Y. She, S. Wang, C. Zhang, H. Li, F. Jin, M. Jin and J. Wang, SERS-active metal–organic frameworks with embedded gold nanoparticles, *Analyst*, 2017, **142**, 2640–2647.

54 J. Feng, H. Lu, Y. Yang, W. Huang, H. Cheng, H. Kong and L. Li, SERS-ELISA determination of human carboxylesterase 1 using metal–organic framework doped with gold nanoparticles as SERS substrate, *Mikrochim. Acta*, 2021, **188**, 280.

55 Y. Hu, H. Cheng, X. Zhao, J. Wu, F. Muhammad, S. Lin, J. He, L. Zhou, C. Zhang, Y. Deng, P. Wang, Z. Zhou, S. Nie and H. Wei, Surface-Enhanced Raman Scattering Active Gold Nanoparticles with Enzyme-Mimicking Activities for Measuring Glucose and Lactate in Living Tissues, *ACS Nano*, 2017, **11**, 5558–5566.

56 Y. Jiang, Y. Cai, S. Hu, X. Guo, Y. Ying, Y. Wen, Y. Wu and H. Yang, Construction of Au@Metal-organic framework for sensitive determination of creatinine in urine, *J. Innovative Opt. Health Sci.*, 2021, **14**, 2141003.

57 X. Kuang, S. Ye, X. Li, Y. Ma, C. Zhang and B. Tang, A new type of surface-enhanced Raman scattering sensor for the enantioselective recognition of D/L-cysteine and D/L-asparagine based on a helically arranged Ag NPs@homo-chiral MOF, *Chem. Commun.*, 2016, **52**, 5432–5435.

58 C. S. L. Koh, H. Y. F. Sim, S. X. Leong, S. K. Boong, C. Chong and X. Y. Ling, Plasmonic Nanoparticle-Metal–Organic Framework (NP-MOF) Nanohybrid Platforms for Emerging Plasmonic Applications, *ACS Mater. Lett.*, 2021, **3**, 557–573.

59 Z. Jiang, P. Gao, L. Yang, C. Huang and Y. Li, Facile in Situ Synthesis of Silver Nanoparticles on the Surface of Metal–Organic Framework for Ultrasensitive Surface-Enhanced Raman Scattering Detection of Dopamine, *Anal. Chem.*, 2015, **87**, 12177–12182.

60 Z. J. Sun, Z. W. Jiang and Y. F. Li, Poly(dopamine) assisted in situ fabrication of silver nanoparticles/metal–organic framework hybrids as SERS substrates for folic acid detection, *RSC Adv.*, 2016, **6**, 79805–79810.

61 A. Zhu, T. Wang, Y. Jiang, S. Hu, W. Tang, X. Liu, X. Guo, Y. Ying, Y. Wu, Y. Wen and H. Yang, SERS determination of dopamine using metal–organic frameworks decorated with Ag/Au noble metal nanoparticle composite after azo derivatization with p-aminothiophenol, *Mikrochim. Acta*, 2022, **189**, 207.

62 S. Hu, Y. Jiang, Y. Wu, X. Guo, Y. Ying, Y. Wen and H. Yang, Enzyme-Free Tandem Reaction Strategy for Surface-Enhanced Raman Scattering Detection of Glucose by Using the Composite of Au Nanoparticles and Porphyrin-Based Metal–Organic Framework, *ACS Appl. Mater. Interfaces*, 2020, **12**, 55324–55330.

63 X. Kuang, S. Ye, X. Li, Y. Ma, C. Zhang and B. Tang, A new type of surface-enhanced Raman scattering sensor for the enantioselective recognition of D/L-cysteine and D/L-asparagine based on a helically arranged Ag NPs@homo-chiral MOF, *Chem. Commun.*, 2016, **52**, 5432–5435.

64 H. Li, W. Geng, S. A. Haruna, M. M. Hassan and Q. Chen, A target-responsive release SERS sensor for sensitive detection of tetracycline using aptamer-gated HP-Uio-66-NH(2) nanochannel strategy, *Anal. Chim. Acta*, 2022, **1220**, 339999.

65 N. Huo, D. Li, S. Zheng and W. Deng, MOF-based hybrid film for multiphase detection of sulfur dioxide with colorimetric and surface-enhanced Raman scattering readout, *Chem. Eng. J.*, 2022, **432**, 134317.

66 A. Das, N. Choi, J.-I. Moon and J. Choo, Determination of total iron-binding capacity of transferrin using metal organic framework-based surface-enhanced Raman scattering spectroscopy, *J. Raman Spectrosc.*, 2021, **52**, 506–515.

67 G. Qi, J. Wang, K. Ma, Y. Zhang, J. Zhang, W. Xu and Y. Jin, Label-Free Single-Particle Surface-Enhanced Raman Spectroscopy Detection of Phosphatidylserine Externalization on Cell Membranes with Multifunctional Micron-Nano Composite Probes, *Anal. Chem.*, 2021, **93**, 2183–2190.

68 Q. Shao, D. Zhang, C.-E. Wang, Z. Tang, M. Zou, X. Yang, H. Gong, Z. Yu, S. Jin and P. Liang, Ag@MIL-101(Cr) Film Substrate with High SERS Enhancement Effect and Uniformity, *J. Phys. Chem. C*, 2021, **125**, 7297–7304.

69 L. He, Y. Liu, J. Liu, Y. Xiong, J. Zheng, Y. Liu and Z. Tang, Core–Shell Noble-Metal@Metal-Organic-Framework Nanoparticles with Highly Selective Sensing Property, *Angew. Chem., Int. Ed.*, 2013, **52**, 3741–3745.

70 Y. Zhang, Y. Hu, G. Li and R. Zhang, A composite prepared from gold nanoparticles and a metal organic framework

(type MOF-74) for determination of 4-nitrothiophenol by surface-enhanced Raman spectroscopy, *Mikrochim. Acta*, 2019, **186**, 477.

71 P. Fuchs, C. Loeseken, J. K. Schubert and W. Miekisch, Breath gas aldehydes as biomarkers of lung cancer, *Int. J. Cancer*, 2010, **126**, 2663–2670.

72 C. Rascón and A. O. Parry, Geometry-dominated fluid adsorption on sculpted solid substrates, *Nature*, 2000, **407**, 986–989.

73 M. K. Khaing Oo, Y. Guo, K. Reddy, J. Liu and X. Fan, Ultrasensitive Vapor Detection with Surface-Enhanced Raman Scattering-Active Gold Nanoparticle Immobilized Flow-Through Multihole Capillaries, *Anal. Chem.*, 2012, **84**, 3376–3381.

74 E.-C. Lin, J. Fang, S.-C. Park, F. W. Johnson and H. O. Jacobs, Effective localized collection and identification of airborne species through electrodynamic precipitation and SERS-based detection, *Nat. Commun.*, 2013, **4**, 1636.

75 L. J. Murray, M. Dinca and J. R. Long, Hydrogen storage in metal-organic frameworks, *Chem. Soc. Rev.*, 2009, **38**, 1294–1314.

76 T. Wang, J. Zhuang, J. Lynch, O. Chen, Z. Wang, X. Wang, D. LaMontagne, H. Wu, Z. Wang and Y. C. Cao, Self-Assembled Colloidal Superparticles from Nanorods, *Science*, 2012, **338**, 358–363.

77 H. Sun, B. Yu, X. Pan, X. Zhu and Z. Liu, Recent progress in metal-organic frameworks-based materials toward surface-enhanced Raman spectroscopy, *Appl. Spectrosc. Rev.*, 2022, **57**, 513–528.

78 J. Deng, K. Wang, M. Wang, P. Yu and L. Mao, Mitochondria Targeted Nanoscale Zeolitic Imidazole Framework-90 for ATP Imaging in Live Cells, *J. Am. Chem. Soc.*, 2017, **139**, 5877–5882.

79 L. He, M. Brasino, C. Mao, S. Cho, W. Park, A. P. Goodwin and J. N. Cha, DNA-Assembled Core-Satellite Upconverting-Metal-Organic Framework Nanoparticle Superstructures for Efficient Photodynamic Therapy, *Small*, 2017, **13**, 1700504.

80 X. Chen, L. Qin, S.-Z. Kang and X. Li, A special zinc metal-organic frameworks-controlled composite nanosensor for highly sensitive and stable SERS detection, *Appl. Surf. Sci.*, 2021, **550**, 149302.

81 H. Sun, S. Cong, Z. Zheng, Z. Wang, Z. Chen and Z. Zhao, Metal-Organic Frameworks as Surface Enhanced Raman Scattering Substrates with High Tailorability, *J. Am. Chem. Soc.*, 2019, **141**, 870–878.

82 O. Guselnikova, H. Lim, J. Na, M. Eguchi, H. J. Kim, R. Elashnikov, P. Postnikov, V. Svorcik, O. Semyonov, E. Miliutina, O. Lyutakov and Y. Yamauchi, Enantioselective SERS sensing of pseudoephedrine in blood plasma biomatrix by hierarchical mesoporous Au films coated with a homochiral MOF, *Biosens. Bioelectron.*, 2021, **180**, 113109.

83 X. Chen, Y. Zhang, X. Kong, K. Yao, L. Liu, J. Zhang, Z. Guo, W. Xu, Z. Fang and Y. Liu, Photocatalytic Performance of the MOF-Coating Layer on SPR-Excited Ag Nanowires, *ACS Omega*, 2021, **6**, 2882–2889.

84 M. Sen Bishwas, M. Malik and P. Poddar, Raman spectroscopy-based sensitive, fast and reversible vapour phase detection of explosives adsorbed on metal-organic frameworks UiO-67, *New J. Chem.*, 2021, **45**, 7145–7153.

85 Z. Lei, C. Dai and B. Chen, Gas solubility in ionic liquids, *Chem. Rev.*, 2014, **114**, 1289–1326.

86 K. Okamoto, I. Niki, A. Shvartser, Y. Narukawa, T. Mukai and A. Scherer, Surface-plasmon-enhanced light emitters based on InGaN quantum wells, *Nat. Mater.*, 2004, **3**, 601–605.

87 J. Xu, S. Shang, W. Gao, P. Zeng and S. Jiang, Ag@ZIF-67 decorated cotton fabric as flexible, stable and sensitive SERS substrate for label-free detection of phenol-soluble modulin, *Cellulose*, 2021, **28**, 7389–7404.

88 O. Guselnikova, H. Lim, J. Na, M. Eguchi, H.-J. Kim, R. Elashnikov, P. Postnikov, V. Svorcik, O. Semyonov, E. Miliutina, O. Lyutakov and Y. Yamauchi, Enantioselective SERS sensing of pseudoephedrine in blood plasma biomatrix by hierarchical mesoporous Au films coated with a homochiral MOF, *Biosens. Bioelectron.*, 2021, **180**, 113109.

89 X. Xu and X. Wang, Perovskite Nano-Heterojunctions: Synthesis, Structures, Properties, Challenges, and Prospects, *Small Struct.*, 2020, **1**, 2000009.

90 L. Du, B. Zhang, W. Deng, Y. Cheng, L. Xu and L. Mai, Hierarchically Self-Assembled MOF Network Enables Continuous Ion Transport and High Mechanical Strength, *Adv. Energy Mater.*, 2022, **12**, 2200501.

91 F. Ahmadijokani, R. Mohammadkhani, S. Ahmadipouya, A. Shokrgozar, M. Rezakazemi, H. Molavi, T. M. Aminabhavi and M. Arjmand, Superior chemical stability of UiO-66 metal-organic frameworks (MOFs) for selective dye adsorption, *Chem. Eng. J.*, 2020, **399**, 125346.

92 H. Wu, Y. S. Chua, V. Krungleviciute, M. Tyagi, P. Chen, T. Yildirim and W. Zhou, Unusual and Highly Tunable Missing-Linker Defects in Zirconium Metal-Organic Framework UiO-66 and Their Important Effects on Gas Adsorption, *J. Am. Chem. Soc.*, 2013, **135**, 10525–10532.

93 B. Li, M. Chrzanowski, Y. Zhang and S. Ma, Applications of metal-organic frameworks featuring multi-functional sites, *Coord. Chem. Rev.*, 2016, **307**, 106–129.

94 J. Park, Y. S. Chae, D. W. Kang, M. Kang, J. H. Choe, S. Kim, J. Y. Kim, Y. W. Jeong and C. S. Hong, Shaping of a Metal-Organic Framework-Polymer Composite and Its CO₂ Adsorption Performances from Humid Indoor Air, *ACS Appl. Mater. Interfaces*, 2021, **13**, 25421–25427.

95 E. González-Zamora and I. A. Ibarra, CO₂ capture under humid conditions in metal-organic frameworks, *Mater. Chem. Front.*, 2017, **1**, 1471–1484.

96 S. Bhattacharyya, R. Han, W.-G. Kim, Y. Chiang, K. C. Jayachandrababu, J. T. Hungerford, M. R. Dutzer, C. Ma, K. S. Walton, D. S. Sholl and S. Nair, Acid Gas Stability of Zeolitic Imidazolate Frameworks: Generalized Kinetic and Thermodynamic Characteristics, *Chem. Mater.*, 2018, **30**, 4089–4101.

97 L. Huang, Y. Zhu, C. Xu, Y. Cai, Y. Yi, K. Li, X. Ren, D. Jiang, Y. Ge, X. Liu, W. Sun, Q. Zhang and Y. Wang, Noninvasive Diagnosis of Gastric Cancer Based on Breath Analysis with a Tubular Surface-Enhanced Raman Scattering Sensor, *ACS Sens.*, 2022, **7**, 1439–1450.

98 Z. Xia, D. Li and W. Deng, Identification and Detection of Volatile Aldehydes as Lung Cancer Biomarkers by Vapor Generation Combined with Paper-Based Thin-Film Micro-extraction, *Anal. Chem.*, 2021, **93**, 4924–4931.

99 K. Yang, S. Zong, Y. Zhang, Z. Qian, Y. Liu, K. Zhu, L. Li, N. Li, Z. Wang and Y. Cui, Array-Assisted SERS Microfluidic Chips for Highly Sensitive and Multiplex Gas Sensing, *ACS Appl. Mater. Interfaces*, 2020, **12**, 1395–1403.

100 D. Xie, R. Wang, J. Fu, Z. Zhao and M. Li, AuNPs@MIL-101(Cr) as a SERS-Active Substrate for Sensitive Detection of VOCs, *Front. Bioeng. Biotechnol.*, 2022, **10**, 921693.

101 Y. Huang, T. Xie, K. Zou, Y. Gu, G. Yang, F. Zhang, L.-L. Qu and S. Yang, Ultrasensitive SERS detection of exhaled biomarkers of lung cancer using a multifunctional solid phase extraction membrane, *Nanoscale*, 2021, **13**, 13344–13352.

102 H. Lu, Y. Yang, R. Chen, W. Huang, H. Cheng, X. Liu, H. Kong, L. Li and J. Feng, Quantitative evaluation of human carboxylesterase 1 by SERS-ELISA using a synergistic enhancement strategy based on gold nanoparticles and metal-organic framework, *Microchem. J.*, 2022, **183**, 108114.

103 Y. Wu, J.-Y. Chen and W.-M. He, Surface-enhanced Raman spectroscopy biosensor based on silver nanoparticles@metal-organic frameworks with peroxidase-mimicking activities for ultrasensitive monitoring of blood cholesterol, *Sens. Actuators, B*, 2022, **365**, 131939.

104 Z. Yang, T. Liu, W. Wang and L. Zhang, Stacked hexagonal prism of Ag@Ni-MOF-1 as functionalized SERS platform through rational integration of catalytic synthesis of dopamine-quinone at physiological pH with a biomimetic route, *Chem. Commun.*, 2020, **56**, 3065–3068.

105 Y. He, Y. Wang, X. Yang, S. Xie, R. Yuan and Y. Chai, Metal Organic Frameworks Combining CoFe₂O₄ Magnetic Nanoparticles as Highly Efficient SERS Sensing Platform for Ultrasensitive Detection of N-Terminal Pro-Brain Natriuretic Peptide, *ACS Appl. Mater. Interfaces*, 2016, **8**, 7683–7690.

106 J. He, J. Dong, Y. Hu, G. Li and Y. Hu, Design of Raman tag-bridged core-shell Au@Cu₃(BTC)₂ nanoparticles for Raman imaging and synergistic chemo-photothermal therapy, *Nanoscale*, 2019, **11**, 6089–6100.

107 C. Carrillo-Carrión, R. Martínez, M. F. Navarro Poupart, B. Pelaz, E. Polo, A. Arenas-Vivo, A. Olgiati, P. Taboada, M. G. Soliman, Ú. Catalán, S. Fernández-Castillejo, R. Solà, W. J. Parak, P. Horcajada, R. A. Alvarez-Puebla and P. del Pino, Aqueous Stable Gold Nanostar/ZIF-8 Nanocomposites for Light-Triggered Release of Active Cargo Inside Living Cells, *Angew. Chem., Int. Ed.*, 2019, **58**, 7078–7082.

108 P. Jiang, Y. Hu and G. Li, Biocompatible Au@Ag nanorod@ZIF-8 core-shell nanoparticles for surface-enhanced Raman scattering imaging and drug delivery, *Talanta*, 2019, **200**, 212–217.

109 X. Chen, F. Xu, Y. Wang, Y. Pan, D. Lu, P. Wang, K. Ying, E. Chen and W. Zhang, A study of the volatile organic compounds exhaled by lung cancer cells in vitro for breath diagnosis, *Cancer*, 2007, **110**, 835–844.

110 N. Peled, O. Barash, U. Tisch, R. Ionescu, Y. Y. Broza, M. Ilouze, J. Mattei, P. A. Bunn, F. R. Hirsch and H. Haick, Volatile fingerprints of cancer specific genetic mutations, *Nanomedicine*, 2013, **9**, 758–766.

111 M. Phillips, N. Altorki, J. H. M. Austin, R. B. Cameron, R. N. Cataneo, R. Kloss, R. A. Maxfield, M. I. Munawar, H. I. Pass, A. Rashid, W. N. Rom, P. Schmitt and J. Wai, Detection of lung cancer using weighted digital analysis of breath biomarkers, *Clin. Chim. Acta*, 2008, **393**, 76–84.

112 G. Song, T. Qin, H. Liu, G. B. Xu, Y. Y. Pan, F. X. Xiong, K. S. Gu, G. P. Sun and Z. D. Chen, Quantitative breath analysis of volatile organic compounds of lung cancer patients, *Lung Cancer*, 2010, **67**, 227–231.

113 J. Kneipp, H. Kneipp and K. Kneipp, SERS—a single-molecule and nanoscale tool for bioanalytics, *Chem. Soc. Rev.*, 2008, **37**, 1052–1060.

114 J. S. Rodríguez-Zavala, L. F. Calleja, R. Moreno-Sánchez and B. Yoval-Sánchez, Role of Aldehyde Dehydrogenases in Physiopathological Processes, *Chem. Res. Toxicol.*, 2019, **32**, 405–420.

115 S. Singh, C. Brocker, V. Koppaka, Y. Chen, B. C. Jackson, A. Matsumoto, D. C. Thompson and V. Vasiliou, Aldehyde dehydrogenases in cellular responses to oxidative/electrophilic stress, *Free Radical Biol. Med.*, 2013, **56**, 89–101.

116 S. Reuter, S. C. Gupta, M. M. Chaturvedi and B. B. Aggarwal, Oxidative stress, inflammation, and cancer: How are they linked?, *Free Radical Biol. Med.*, 2010, **49**, 1603–1616.

117 Q. Ding, J. Wang, X. Chen, H. Liu, Q. Li, Y. Wang and S. Yang, Quantitative and Sensitive SERS Platform with Analyte Enrichment and Filtration Function, *Nano Lett.*, 2020, **20**, 7304–7312.

118 E. E. Ahi, H. Torul, A. Zengin, F. Sucularlı, E. Yıldırım, Y. Selbes, Z. Suludere and U. Tamer, A capillary driven microfluidic chip for SERS based hCG detection, *Biosens. Bioelectron.*, 2022, **195**, 113660.

119 Z. Huang, A. Zhang, Q. Zhang and D. Cui, Nanomaterial-based SERS sensing technology for biomedical application, *J. Mater. Chem. B*, 2019, **7**, 3755–3774.

120 X. Fan, W. Ming, H. Zeng, Z. Zhang and H. Lu, Deep learning-based component identification for the Raman spectra of mixtures, *Analyst*, 2019, **144**, 1789–1798.